NATIONAL ADVISORY COMMITTEE FOR AERONAUTICS

TECHNICAL NOTE

No. 1483

FLIGHT MEASUREMENTS OF AERODYNAMIC LOADS ON THE HORIZONTAL TAIL SURFACE OF A FIGHTER-TYPE AIRPLANE

By John B. Garvin

Langley Memorial Aeronautical Laboratory
Langley Field, Va.

Washington
November 1947

NATIONAL ADVISORY COMMITTEE FOR AERONAUTICS

TECHNICAL NOTE NO. 1483

FLIGHT MEASUREMENTS OF AERODYNAMIC LOADS ON THE HORIZONTAL TAIL SURFACE OF A FIGHTER-TYPE AIRPLANE

By John B. Garvin

SUMMARY

A comprehensive investigation was conducted to determine the loads applied to the horizontal tail surface of a fighter-type airplane in maneuvering flight. Differential-pressure-distribution methods were employed to obtain the values of load. Loads were measured at equivalent airspeeds ranging from 125 to 380 miles per hour and at accelerations up to 6g. Engine power and sideslip conditions were also varied during the tests. The data were analyzed along theoretical lines to determine the parameters affecting the tail load and to indicate the contribution of speed, normal acceleration, and angular acceleration to the total tail load and the contribution of power condition and sideslip to the load dissymmetry. The test data have been prepared in both tabular and graphical form and several typical time histories of chordwise and spanwise load distribution are included.

The flight-test results verify the fact that the accurate determination of the tail-load parameters will permit the calculation of the horizontal-tail load for various conditions of speed and normal and angular acceleration. These parameters are the pitching-moment coefficient, the location of the aerodynamic center of the airplane without the horizontal tail, and the pitching angular acceleration.

In a sideslip the upwind tail surface experienced an up-load increment relative to the downwind tail surface. As would be expected from a consideration of the reasons for load unbalance between the two sides of the horizontal tail, the load dissymmetry was applied mainly to the stabilizer surface with only a small part carrying over to the elevators.

The conditions of critical design loads are shown to occur at high values of pitching angular acceleration in combination with high positive load factors and medium speed for the up direction or high negative load factors and maximum speed for the down direction. The tail-load increment caused by pitching angular acceleration is confined principally to the elevator surfaces.

INTRODUCTION

A flight investigation was made of the aerodynamic loads exerted on the horizontal tail surfaces of a fighter-type airplane in order to determine the maneuvering design tail-load criterions. The measurements considered most important were those which gave the magnitude and distribution of the aerodynamic load over the horizontal stabilizer and elevators as well as a time history of the motion of the airplane resulting from a given elevator deflection. Accordingly, measurements were made of the horizontal-tail load and of the motions of the airplane in abrupt pitching maneuvers in which the following quantities were varied: initial airspeed, airplane load factor, power condition, rate of control-surface motion, amount of control-surface motion, and angle of sideslip. This paper presents the results obtained in these tests and gives an analysis of the data such as to indicate the horizontal-tail loads associated with pitching maneuvers of the test airplane. Since the number of variables that occur in the tail-load problem is large, the isolation of any one variable is difficult; therefore, the data are given in several forms such as tables, graphs, and typical time histories of maneuvers. The data have been analyzed theoretically to indicate the contribution of speed, normal acceleration, and angular acceleration to the total tail load and the contribution of power and sideslip to the tail-load dissymmetry.

SYMBOLS

W airplane weight, pounds

g acceleration of gravity, feet per second per second

S area, square feet

x_t distance from aerodynamic center of airplane without horizontal tail to aerodynamic center of horizontal tail, negative quantity, feet

D propeller diameter, feet

I_Y pitching moment of inertia, slug-feet^2

V_e equivalent airspeed, miles per hour $\left(V\sigma^{1/2}\right)$

V true airspeed, miles per hour

d distance from center of gravity of airplane to aerodynamic center of airplane without horizontal tail, negative quantity, feet

ρ	mass density of air, slugs per cubic foot
σ	density ratio of air
q	dynamic pressure, pounds per square foot
L	load (up load, positive), pounds
C_L	airplane lift coefficient, assumed equal to the normal force coefficient $\left(n_{c.g.}W/qS_w\right)$
N	engine speed, revolutions per minute
P	brake horsepower
$\bar{c}$	mean aerodynamic chord
Q_c	torque coefficient $\left(33{,}000P/2\pi N\rho V^2D^3\right)$
M	Mach number
p	differential pressure, pounds per square foot
δ	control deflection (positive, trailing edge down), degrees
θ	angle of pitch, degrees
β	angle of sideslip, degrees
ζ	angle of flow near horizontal tail, degrees
n	normal load factor
F	stick force, pounds
C_m	pitching-moment coefficient of airplane less tail (Pitching moment/$qS\bar{c}$)
$C_{\Delta N_t}$	tail-load-dissymmetry coefficient $\left(\dfrac{L_{t_L} - L_{t_R}}{qS_t}\right)$

Subscripts:

c.g.	center of gravity
R	right
L	left

max maximum value

e elevator

t tail

w wing

APPARATUS

Airplane.- The pertinent characteristics and a three-view drawing of the fighter-type airplane tested are given in figure 1. When the airplane was prepared for flight tests, slight changes were made in its construction and arrangement to facilitate the installation of adequate instruments and to provide the necessary strength and balance to permit safe operation. The horizontal tail surface was of the same contour and plan form as the standard tail surface of the production airplane but was equipped with 260 flush-mounted static orifices distributed over the upper and lower surfaces of both the stabilizer and elevator in the locations shown in figure 2. These orifices were attached to individual pressure tubes which were grouped into bundles inside the tail surfaces and were run inboard to a point near the fuselage where a cut-out was placed to permit exit of the tube bundles under an enlarged fairing at the stabilizer-fuselage junction.

Instruments.- Differential pressures were measured over the tail surface with two 60-cell multiple photographically recording manometers which were installed in the approximate location of the fuselage fuel tank. In addition to the manometers, the airplane was equipped with the following standard recording instruments:

One NACA airspeed recorder connected to a freely swiveling static head mounted on a boom at approximately one chord length ahead of the right wing tip and connected to a shielded total head mounted on the boom. Both of these heads were little affected by angles of yaw up to 20°.

Two NACA three-component accelerometers, one mounted 74.8 inches and the other 175.8 inches rearward of the leading edge of the mean aerodynamic chord.

One NACA pitching-angular-velocity recorder.

Two NACA electrical control-position recorders mounted to record the position of the elevator and the rudder near the juncture of these two surfaces.

One NACA control-force recorder mounted to measure the elevator stick forces.

One NACA angle-of-flow recorder located near the horizontal tail surface mounted to measure vertical flow angles. The head was 15 inches forward of and 16.5 inches below the leading edge of orifice row C_R (fig. 2).

One NACA sideslip-angle recorder mounted forward of the left wing tip. This instrument was mounted for only a few tests of this investigation.

One NACA synchronizing timer to give time pulse intervals of 0.1 second.

FLIGHT TESTS

The effects of such variables as airspeed, acceleration, power, center-of-gravity position, angle of sideslip, and the amount and rate of elevator motion on the tail load were determined by measuring the tail load in both steady and maneuvering flight.

Steady-flight tests.- In these tests, which were also used for airspeed calibrations, a number of short runs were made both in steady straight flight at 1g and in steady turns. The range of conditions covered was as follows:

Equivalent airspeed, 125 to 300 miles per hour
Power condition, power off to sufficient power for steady level flight
Center-of-gravity position, 28 percent to 33.5 percent mean aerodynamic chord
Normal acceleration, steady turns at approximately 2g, 2.5g, and 3g

The short steady-flight part of each maneuver also served as steady-flight material. For each run the following quantities were measured:

Indicated airspeed
Normal acceleration at the center of gravity
Angle of flow near right horizontal tail surface
Elevator position relative to stabilizer chord line
Aerodynamic load imposed on the various parts of the horizontal tail surface

Maneuvering-flight tests.- The loads applied on the horizontal tail surfaces were measured in the following maneuvers:

Abrupt pull-ups from steady flight at equivalent airspeeds varying from 125 to 380 miles per hour, both with power off and with sufficient power for level flight. Runs made with power on at speeds in excess of the level-flight speed were made in a shallow glide with rated power.

Abrupt pull-ups as preceding, but at varying rates of control deflection. The rates of deflection were determined arbitrarily by the pilot to be fast, medium, or slow.

Abrupt pull-ups from steady flight in which varying amounts of sideslip to the left and right were obtained prior to the execution of the maneuver.

In most of the maneuvering-flight tests, the runs were made below an altitude of 10,000 feet, but one series of stalled pull-ups was made at 25,000 feet. The center of gravity of the airplane, in the maneuvering tests, was at either 29.7 or 30.6 percent mean aerodynamic chord.

In addition to the items listed under steady flight the following quantities were measured or evaluated:

Pitching angular velocity
Maximum positive pitching angular acceleration
Maximum rate of elevator deflection
Angle of sideslip (when intentional sideslips were made)
Elevator stick force
Normal acceleration near the tail surface

METHOD AND RESULTS

For the maneuvering-flight tests sufficient points were read on the flight records so that a time variation of all the pertinent quantities could be established. In each run of the steady-flight tests all records were read at the same instant. In order to obtain the tail loads, the point differential pressures were first read and plotted and from these values the spanwise distribution and the total tail load were determined by graphical integration methods.

Since the number of independent variables which enter into the tail-load problem cannot be completely controlled in a given test, complete isolation of the effect of any one variable was unpracticable. The test results are therefore presented in several forms, such as tables, graphs, and typical time histories of the various quantities in order to give a better picture of the tail-load variation.

The complete results of the steady-flight runs are given in table I. The weights given allow for gas consumption; the horsepower was determined from the pilot's notation of engine speed, manifold pressure, pressure altitude, and free-air temperature, and by use of the performance charts prepared by the Allison Division of the General Motors Corporation. The torque coefficient Q_c was computed from the formula given in the "SYMBOLS." The value of the elevator angle δ_e corresponds to that required for trim under the conditions tested; down angles are taken as positive. The angle of flow ζ is the angle between the stabilizer chord line and the air stream at the location of the NACA angle-of-flow recorder. The dynamic pressure q was used with the load factor $n_{c.g.}$ to compute the airplane lift coefficient. The integrated tail load expressed in pounds with upward-acting loads taken as positive is also given in table I.

Similarly, all the data obtained in the pull-ups are summarized in table II which contains the measurements for each run at the following particular time points: the time of steady flight prior to the start of the maneuver, the time of maximum incremental down tail load, the time of maximum normal center-of-gravity acceleration, and the time of maximum incremental up tail load. The time values of table II are given in the preceding order irrespective of their actual sequence. A number of headings in this table are similar to those in table I; however, data have been added including the values of the equivalent airspeed V_e, the load factor at the tail n_t, the elevator stick force F_e, the pitching angular velocity $\dot{\theta}$, and the initial sideslip angle β. The horizontal tail loads on both the right and left sides of the elevator and stabilizer are given separately. For analysis the maximum positive pitching angular acceleration $\ddot{\theta}_{max}$ and the maximum rate of elevator movement $\dot{\delta}_{e_{max}}$ are also given in table II. These quantities are the maximum values measured near the start of the maneuver and do not necessarily correspond to any of the time intervals given.

The values given in table II were compiled from time variations such as are shown in figures 3 to 14 for typical pull-up maneuvers. Differences between the stalled and unstalled pull-up are shown in figures 3 to 5. The effects of power on the measurements are illustrated in figures 6 to 8. The effect of initial right and left sideslip on the measured tail loads for the power-on condition is shown in figures 9 to 11 and similar results for the power-off condition are shown in figures 12 to 14.

Isometric views of the differential pressure distribution over the stabilizer and elevators are given in figures 15 and 16 for the maneuvers of the time variations of figures 3 and 9. Typical spanwise load distributions over the horizontal tail are shown in figures 17 and 18 for four selected pull-up maneuvers. The times were selected arbitrarily to give an idea of the magnitude and distribution of load as it varied during the pull-up maneuver. The change in load distribution caused by the addition of power is shown in figure 17 and the effects of right and left sideslip on the spanwise load distribution are shown in figure 18.

ACCURACY

An estimate of the accuracy of the measurements made in this investigation is given as follows:

Dynamic pressure, pounds per square foot	±3
Acceleration at center of gravity, g	±0.1
Pitching angular acceleration, radian per second per second	±0.2
Control position, degree	±0.3
Stick force, pounds	±4
Tail angle of flow, degrees	±2
Tail load, pounds (The accuracy of the incremental tail-load measurements during any given test was greater than ±50 lb)	±50
Brake horsepower	±100
Time, second	±0.05
Altitude, feet	±200
Pitching angular velocity, radian per second	±0.02
Yaw angle, degrees	±2
Center-of-gravity position, percent mean aerodynamic chord	±0.1

ANALYSIS OF RESULTS

The results compiled in tables I and II were analyzed first by considering the total aerodynamic tail loads imposed upon the airplane, and then by considering the parts of this load imposed upon the right half and left half of the horizontal tail during various flight conditions.

Total tail load.- The total tail load which the airplane experienced at any time was considered to be composed of three parts: a part L_1 required to balance the pitching moments of the wing, fuselage, and propeller in a zero-lift dive, termed the "zero-lift tail load;" a part L_2 required to balance the pitching moments of the airplane weight and normal inertia, termed the "normal-acceleration tail load;" and a part L_3 required to balance the airplane pitching angular inertia, termed the "pitching-angular-acceleration tail load." The total aerodynamic tail load in equation form is

$$L_t = \underbrace{-\frac{C_m q S \bar{c}}{x_t}}_{L_1} + \underbrace{\frac{n_{c.g.} W d}{x_t}}_{L_2} + \underbrace{\frac{I_Y \ddot{\theta}}{x_t}}_{L_3} \tag{1}$$

The various parts of this equation are illustrated in figure 19 for a hypothetical pull-up. It is obvious from equation (1) that, for a given airplane, L_1 will depend upon C_m, q, and x_t, and therefore would be expected to be a function of the dynamic pressure and Mach number. The load L_2 will be a function of the load factor, center-of-gravity position, and Mach number as it affects d and x_t. The load L_3 will depend principally upon the pitching angular acceleration $\ddot{\theta}$ which, like the load factor n, is a function of the manner in which the pilot manipulates the elevator controls in a particular maneuver.

The determination of the maneuvering tail load requires a knowledge of the various factors of equation (1) which apply for the given airplane. In the case of the subject airplane these factors were not known. The flight test data given in tables I and II, however, furnished a means for evaluating some of the factors and permitted the determination of the others. Once the quantities were evaluated they could then be extrapolated for values beyond the range of the test conditions.

The aerodynamic-center location occurring in equation (1) was found by differentiating that equation with respect to load factor n with all other terms assumed constant. Thus,

$$x_t = \frac{Wd}{dL_t/dn_{c.g.}} \tag{2}$$

But, by definition,

$$x_t = d + l \tag{3}$$

where l is the distance from the center of gravity of the airplane to the aerodynamic center of the tail. By use of the steady-level-flight and steady-turning-flight data of tables I and II, as shown in figure 20, a value for $\frac{dL_t}{dn} = 390$ pounds per g was found which when substituted into equations (2) and (3) gave an aerodynamic-center location at 17.5 percent mean aerodynamic chord.

The determination of the pitching-moment coefficient for the airplane less tail C_m was found by differentiating equation (1) with respect to dynamic pressure q, with all other terms assumed constant. Thus,

$$C_m = -\frac{dL_t}{dq}\frac{x_t}{S\bar{c}} \tag{4}$$

Values for $\frac{dL_t}{dq}$ were determined from the steady-level-flight data shown in figure 20 and were found to be -5.2 and -4.72 pounds per pound per square foot for the power-on and power-off conditions, respectively. The substitution of these values into equation (4) gave a value of C_m of -0.0552 for the power-on and -0.0501 for the power-off condition.

By use of the values of C_m, d, and x_t it is possible to determine the tail load which would be required to balance the airplane in any steady flight condition (that is, for $\dot{\theta} = 0$) even beyond the conditions tested. Figure 21 contains curves of L_1 for the test airplane against the equivalent airspeed for sea level and for 30,000 feet. The value of C_m used in the determination of L_1 in this figure has been corrected for Mach number effects according to $C_m = \frac{-0.0552(\text{or } -0.0501)}{\sqrt{1 - M^2}}$ even though in the range of the tests the effect of M on C_m was found to be small.

Extrapolation of the flight data has also been done in the case of L_2, the normal-acceleration tail load. Here the evaluation of L_2 for various center-of-gravity positions has been made for the limit-load-factor range of the airplane. The results are shown in figure 22 for an assumed gross weight of 8000 pounds. The value of L_2 for other gross weights would be in direct proportion to those shown. The effect of Mach number on the location of the aerodynamic center of the airplane less tail was not found in these tests and therefore no correction for this effect has been applied in figure 22.

Combining the results given in figures 21 and 22 gives the total tail load which will exist on the airplane during any condition of steady flight. The loads for both a forward and a rearward center-of-gravity location for sea-level altitude are shown in figure 23.

In addition to the steady-flight loads found in the foregoing analysis and shown in figure 23, an important load component remains which must be evaluated in order to provide for all the flight conditions. This load, the pitching-angular-acceleration tail load L_3 of equation (1), is primarily a function of the amount and rate of motion of the control surface. Since the amount and rate of motion are in turn dependent upon airspeed and certain intangible items which depend upon pilot response, the data were analyzed in a general way to determine the principal effects of these quantities. The results shown in figure 24 correlate the initial control motion with a pitching-angular-acceleration tail-load factor denoted by L_3/q. The values shown were obtained from the maximum down-tail load increment given in table II at the start of each abrupt pull-up. In addition, the same values of L_3 have been plotted in figure 25 against the maximum positive pitching angular acceleration $\ddot{\theta}$. The value of $\ddot{\theta}$ for each run was obtained by differentiating the pitching-angular-velocity record. The relationship of of these data with the theoretical expression $\frac{I_Y\ddot{\theta}}{x_t}$ is also shown in figure 25. Here the value of I_Y was taken as 8800 slug-feet^2 which was obtained from swinging tests.

In order to indicate how well the values and the method apply, a comparison of computed and measured total tail loads using values for C_m, x_t, d, and I_Y measured in these tests has been made for two complete maneuvers. These comparisons, which are shown in figure 26 for flight 16a, run 3 and flight 22c, run 2, are for a moderate-speed abrupt pull-up with a large value of up-tail-load increment and a pull-up in which sideslip was present. The values of q, n, and $\ddot{\theta}$ measured during the maneuvers were used in computing values of L_1, L_2, and L_3.

Tail-load dissymmetry.- A determination of the effects of slipstream rotation and sideslip on the dissymmetry of tail load was made from an analysis of the steady and sideslipping runs of table II. The differences in load on the right and left horizontal tail have been plotted against the angle of sideslip in figure 27 for various values of the torque coefficient. The values shown represent a range of wing lift conditions varying from a value of C_L of 0.15 to 0.24. Since little scatter was noted within this range of C_L, an average value equal to 0.20 has been assumed. In order to isolate further the effects of power condition and of sideslip, the tail-load-dissymmetry coefficient $C_{\Delta N_t}$ has been plotted against engine brake horsepower in figure 28 for all the steady-flight runs of table I. The angle of sideslip for these runs was not known exactly, but it was assumed that the angles were in all cases less than ±2°, which would correspond to approximately ±100 pounds of dissymmetry or a value of $C_{\Delta N_t}$ of ±0.02 at a speed of 200 miles per hour.

DISCUSSION

Tables I and II contain all the data which are essential for a coordinated analysis with data from other investigations. The representative material presented in the time-history and analysis figures, however, is more suitable for discussing the effects of various factors on the horizontal-tail load.

Maneuver time histories.- Although the time histories shown in figures 3 to 14 are only a few of the many obtained during the course of the investigation, these few illustrate the time sequence of the more important quantities measured, as well as permit a direct comparison of the results from various types of maneuvers. A comparison of the results shown in figures 3 and 5(a) with those given in figures 4 and 5(b) indicates the tail loads are not of necessity greatest for the high-speed ranges of the airplane. This fact was indicated in the analysis shown in figure 23. The pitching-angular-acceleration tail load which occurs near the beginning of the lower-speed pull-up of figure 5(a) was equal to the initial tail load for the higher-speed pull-up of figure 5(b). The elevator loads follow closely, in time, the motions described by the control surface (figs. 3 to 5). The stabilizer loads, on the other hand, follow a loading cycle more nearly like that indicated by the tail NACA angle-of-flow recorder, with exclusion of the time just after the maneuver is started. At the start of the maneuver the displaced control surface results in a down load on the elevator, which induces a slight initial down load on the stabilizer. The pitching of the airplane resulting from this down load causes an increase in angle of attack of the tail which in turn reduces the initial downward load caused by the elevator. Beyond this point the tail angle of flow and the stabilizer loads are approximately in phase.

The two tail-load time histories of the pull-ups of figures 6 and 7 shown in figure 8 were made from approximately the same initial airspeed and to approximately the same load factor. The main difference between these runs was in the rate of control deflection and consequently in the resultant pitching angular accelerations. As would be expected, from considerations of the control deflection and pitching angular acceleration, the tail load L_3 for the run of figure 7 is greater than that of figure 6. This difference is shown clearly by the down-load values and the peak up-load values of figure 8.

The effects of power on the dissymmetry of load may also be obtained from figure 8; in figure 8(a) power was applied whereas in figure 8(b) the engine was throttled. The load dissymmetry, about 250 pounds, experienced while in the power-on pull-up was carried almost entirely on the stabilizer. The difference in load between the two sides of the tail surface remains almost constant throughout the maneuver. Although in this case the angle of sideslip was not measured, the changes in this angle during the maneuver were thought to be small.

The time histories of figures 9 to 11 for the two pull-ups, where the angle of sideslip varied from 4° left in figure 9 to 5° right in figure 10, indicate that the dissymmetry in steady flight (fig. 11) for these two runs is approximately 575 pounds or about 60 pounds per degree of sideslip. This value is also indicated in figure 27.

The results given in figures 12 to 14 show approximately the same increment in dissymmetry as was shown in the power-on sideslipping pull-ups of figures 9 to 11. In both sets of figures the tail surface to windward has a positive increment of load; that is, in slipping to the left the left tail surface carries a smaller down load than the right tail surface.

The lines shown in the middle of figures 11 and 14 indicate the tail loads for straight (without sideslip) flight. If these values are compared with those existing at the time of steady sideslip prior to the start of the maneuver, slipping to the right or left is found to cause an increase in down tail load. This increase is evidence of a change in pitching-moment coefficient of the airplane. The rotating propeller produces an increment in pitching moment when the airplane sideslips. This pitching-moment increment, however, is reversed for opposite sideslip angles. Since the flight tests on this airplane indicate no load-increment reversal with reversal of sideslip, the test airplane is assumed to exhibit a slight change in pitching moment with sideslip greater than the normal change due to the propeller.

In addition to the preceding specific points noted in figures 3 to 14 the following general information is obtained from all pull-ups of this investigation:

The airspeed remains substantially constant until the time of maximum normal acceleration. A slight decrease in speed is noted, however, before the time of maximum up tail load. This result is in accordance with the assumption usually made in theoretical studies.

The maximum pitching-angular-acceleration tail load occurs at approximately the time of maximum pitching angular acceleration and slightly before the time of maximum elevator deflection. This load acts principally on the elevator whereas the normal-acceleration tail load which occurs at the time of maximum acceleration acts on the stabilizer. Returning the elevator to the trim position before the maximum load factor was reached tended to exaggerate the localization of loads on the elevator and stabilizer.

The pitching-angular-acceleration tail load which occurs at the start of each pull-up is slightly overbalanced by an increment of lift produced on the wings as a result of the pitching of the airplane. The airplane thus experiences no net negative-acceleration increment at the start of each pull-up.

Load distribution.- The chordwise and spanwise distributions of load shown in figures 15 to 18 indicate local irregularities which may be attributed to deformation of the surfaces and to irregular flow conditions which occur in the region of the tail.

The reduction in the peak differential pressures over the inboard ribs shown in figures 15 and 16 occurs as a result of the fuselage boundary layer and local interferences which exist at this inboard station. At the time just prior to the maneuver, the differential pressure distribution is seen from figures 15 and 16 to be an angle-of-attack type distribution for the entire tail surface. As soon as the elevator is deflected (parts (b) and (c) of figs. 15 and 16), however, the distribution changes to one which has a maximum pressure differential near the elevator hinge with most of the load increment concentrated on the elevator. In the maximum-up-tail-load condition the distribution finally changes back to an angle-of-attack-type distribution where most of the load is concentrated on the stabilizer (figs. 15(e) and 16(e)). Although neither of the cases shown in figures 15 and 16 contains a complete reversal of the elevator, it can be easily deduced that for such a condition large stabilizer loads and large elevator loads would occur simultaneously in the same direction. This condition would, if performed at the proper speed and load factor, specify a critical loading for the fuselage and tail surface.

The curves of figure 17 show clearly, despite a certain amount of irregularity, the effect of slipstream rotation in producing a difference in load between the two sides of the horizontal tail surface. Although not so clear here as from the time-history figures, the dissymmetry can be seen to remain almost constant throughout the pull-up maneuver. The same type of dissymmetry is shown in figure 18 but in this case the cause of the dissymmetry can be attributed to the sideslipping condition. The tail surface to windward in the sideslip has an up-load increment with respect to the downwind tail surface. The dissymmetry is found to be concentrated mainly on the stabilizer whereas only a slight load difference is supported by the elevators (figs. 5, 8, 11, and 14).

Tail-load parameters.- The quantities C_m, x_t, d, and I_Y required for calculating the tail loads by the method of equation (1) are representative of the pitching moment of the airplane less tail. The greatest net change in this pitching moment will be associated with the design tail loads for the airplane. Generally the quantities C_m, x_t, d, and I_Y either can be found from wind-tunnel tests or can be estimated with a fair degree of accuracy by use of existing engineering procedures. The pitching-moment coefficients were not measured in the wind-tunnel tests of reference 1 but tests of a $\frac{1}{12}$-scale model were available which contained such measurements. These tests of the model gave a value of the pitching-moment coefficient for the airplane less tail and propeller of -0.038. The flight tests gave a value of -0.0501 for the power-off condition. The differences noted are attributed to the presence of the propeller and slight differences between the model and the airplane.

The location of the aerodynamic center, found by use of figure 20 to be at 17.5 percent mean aerodynamic chord, is in agreement with that determined for other fighter-type airplanes. Numerous model tests have shown that the fuselage and the propeller both tend to shift the aerodynamic center forward of the quarter chord point of the mean aerodynamic chord; the amount of shift varies with the particular configuration. Because of the small Mach number range covered by these tests, no shift of the aerodynamic center with increase in Mach number was noted. Shifts of aerodynamic center with Mach number, however, would be an important factor to consider in the tail-load-design problem.

The conditions for which critical loads will be placed upon the airplane tail must be known in order to design the horizontal tail surface. The use of plots such as figures 21 and 22 to obtain the steady-flight tail loads shown in figure 23 requires a knowledge of the parameters C_m, d, and x_t. If these parameters are known for any airplane, the selection of the conditions for critical steady-flight tail loads may easily be made. The largest up tail load will occur with the center of gravity rearward, a large value of airplane load factor, moderate airspeed, and low altitude with power off (fig. 23). The largest down tail load, however, will occur in high-speed power-on flight at high altitude, with a large negative load factor and with rearward center-of-gravity location. The results of the tests substantiate these assumptions.

If the tail loads can be measured in flight, the effective moment of inertia in pitch I_Y can be found (see fig. 25). Alternatively, if the moment of inertia is known, the angular-acceleration tail load can be determined provided the angular acceleration can be assigned It appears from the abrupt pull-ups of present tests that for this airplane an angular acceleration of 3 radians per second per second would seldom be exceeded. As a conservative estimate a maximum value of 5 radians per second per second would seem to suffice for conventional airplanes in the fighter category. An examination of the results given in table II indicates that there is a distinct trend for the maximum angular-acceleration values to decrease as the speed increases. Although in figure 24 the angular-acceleration tail load would appear to increase directly with q, the high-speed pull-up points are associated with the smaller values of elevator angle and L_3/q. For example, a pitching angular acceleration of 4.0 radians per second per second would be associated with a speed of 250 miles per hour; whereas at 400 miles per hour, the value of pitching angular acceleration would be reduced to approximately 0.5 radian per second per second. This decrease is in line with the order of decrease shown for the test airplane. The value of L_3 associated with the pull-up for 250 miles per hour would be approximately 2175 pounds; whereas for the pull-up for 400 miles per hour, the value would be only about 270 pounds.

For the airplane of figure 23 if the pilot were making a 6g pull-up at 225 miles per hour and were to push forward on the stick in checking the maneuver a sufficient amount to obtain a negative pitching acceleration of 2.8 radians per second per second, an up tail load of 3920 pounds would be obtained which would exceed the steady-flight tail-load value for an 8g maneuver at a speed of 250 miles per hour. The agreement between the measured and computed values of tail load shown in figure 26 is considered good since the differences noted between the curves could almost entirely be associated with error of obtaining the pitching angular acceleration by graphical differentiation.

The results shown in figure 27 indicate that the dissymmetry in tail load varies linearly with angle of sideslip. The amount of dissymmetry also appears to increase with torque coefficient in the direction which would be expected from a consideration of the direction of propeller rotation. The wind-tunnel results of reference 1 indicated that the dissymmetry for a value of C_L of 0.2 increased at a rate of about 50 pounds per degree of sideslip and that at zero sideslip the initial dissymmetry would be 150 pounds; whereas a rate of increase of 60 pounds and an initial dissymmetry of 100 pounds are indicated for flight in figure 27.

The scatter of the data in figure 28 for the low-horsepower conditions may be attributed to the inadvertent sideslip angles which were introduced by flight at high lift coefficients. The dissymmetry coefficient values at the higher horsepowers were made at low lift coefficients which would be associated with high-speed flight where angles of sideslip would not vary a great deal. The curves shown in figure 28 represent an estimate of the variation of dissymmetry with power in steady flight for average conditions covering lift-coefficient values of 0 to 0.6 and 0.6 to 1.2.

CONCLUDING REMARKS

The systematic measurement of the loads imposed upon the horizontal tail surface of a fighter-type airplane in maneuvering flight has provided information concerning the variation of load with changes in the important tail-load parameters. The tests verify that the changes in load produced by changes in these parameters are those which would normally be expected from engineering considerations and that an accurate knowledge of the aerodynamic-center location and of the values of the airplane-less-tail pitching-moment coefficient, airspeed, load factor, pitching moment of inertia, and pitching angular acceleration will permit the determination of the horizontal-tail load.

The spanwise distribution of load over the horizontal tail surface is known to be affected by influences which change the distribution of angle of attack across the span. Factors which influence the spanwise angle-of-attack distribution are the power condition or slipstream rotation, the position of the horizontal tail within the slipstream, and the angle of sideslip. The tests indicated that in a sideslip the upwind tail surface carried an up-load increment relative to the downwind surface, and since the load dissymmetry is basically one of angle-of-attack change across the span, most of the dissymmetry appears upon the stabilizer with very little carrying back to the elevators.

In order to design the horizontal tail surface a knowledge of the conditions under which critical loads are applied to the tail surface must be known. Since it must balance other forces applied to the airplane, the tail load will be largest in those conditions of flight for which the net changes in pitching moment are greatest. Such a condition will exist for the up-load case when the airplane is operating with a rearward center-of-gravity position, at minimum speed for maximum load factor, and with power off at sea-level. The critical down-load condition will occur in another flight region where the speed is a maximum with high negative load factors, power on at high altitude. The results of the tests substantiate these assumptions.

Langley Memorial Aeronautical Laboratory
National Advisory Committee for Aeronautics
Langley Field, Va., July 9, 1947

REFERENCE

1. Sweberg, Harold H., and Dingeldein, Richard C.: Effects of Propeller Operation and Angle of Yaw on the Distribution of the Load on the Horizontal Tail Surface of a Typical Pursuit Airplane. NACA ARR No. 4B10, 1944.

TABLE I

STEADY-FLIGHT MEASUREMENTS

Flight	Run	Weight (lb)	bhp	C_Q (a)	$n_{c.g.}$ (g)	C_L	c.g. (percent M.A.C.)	δ_e (deg)	ζ (deg)	q (lb/sq ft)	Horizontal-tail load (lb) Left	Right	Total
4	1	8060	320	0.00674	0.99	0.901	28.0	-3.1	-----	37.5	107	-12	95
4	2	8054	361	.00562	1.03	.717	28.0	-2.9	-----	48.8	88	-47	41
4	3	8048	360	.00409	1.03	.522	28.0	-2.8	-----	67.1	59	-75	-16
4	4	8042	396	.00353	1.03	.409	28.0	-2.4	-----	85.4	-64	-121	-185
4	5	8036	655	.00464	1.08	.337	28.0	-2.0	-----	109.2	-78	-242	-320
4	6	8030	707	.00428	1.06	.279	28.0	-1.8	-----	129.5	-20	-306	-326
4	7	8024	866	.00441	1.06	.234	28.0	-2.4	-----	154.0	-175	-399	-574
4	8	8018	975	.00425	1.05	.204	28.0	-2.5	-----	174.5	-219	-431	-650
4	9	8012	548	.00360	1.00	.287	28.0	-2.3	-----	118.4	-134	-233	-367
4	10	8006	280	.00482	1.07	.816	28.0	-4.0	-----	44.3	88	-24	64
4	11	8006	off		1.09	1.002	28.0	-3.4	-----	36.9	49	84	133
4	12	8005	off		1.01	.412	28.0	-3.9	-----	83.1	-6	-58	-64
4	13	8004	off		1.18	.214	28.0	-2.5	-----	186.4	-319	-285	-604
4	14	----	off		----	----	28.0	----	-----	----	----	----	----
4	15	8060	300	.00503	.96	.724	28.0	-2.5	-----	45.3	77	-37	40
4	16	8054	428	.00536	1.00	.558	28.0	-2.4	-----	60.8	58	-75	-17
4	17	8048	429	.00418	1.03	.448	28.0	-2.3	-----	78.0	31	-123	-92
4	18	8042	525	.00412	1.11	.381	28.0	-1.9	-----	99.0	-78	-184	-262
4	19	8036	670	.00445	1.03	.297	28.0	-1.8	-----	117.5	-107	-277	-384
4	20	8030	820	.00452	1.08	.260	28.0	-1.6	-----	141.5	-157	-352	-509
4	21	8029	off		.94	.922	28.0	-3.5	-----	34.8	67	96	163
4	22	8028	off		.88	.700	28.0	-3.5	-----	42.6	40	65	105
4	23	8027	off		.99	.600	28.0	-3.1	-----	56.0	12	38	50
4	24	8026	off		.98	.552	28.0	-2.8	-----	60.3	-7	18	11
4	25	8025	off		1104	.517	28.0	-2.7	-----	68.6	57	-1	56
4	26	8006	off		.99	.428	28.0	-2.2	-----	78.3	57	-35	22
4	27	8005	off		.98	.354	28.0	-2.1	-----	94.0	-54	-51	-105
4	28	8004	off		.96	.247	28.0	-1.8	-----	131.3	-204	-166	-370
4	29	7972	off		.92	.281	28.0	-1.8	-----	111.0	-165	-75	-240
4	30	7971	off		.98	.231	28.0	-1.5	-----	143.0	-238	-184	-422
4	31	7970	off		.98	.205	28.0	-1.2	-----	161.6	-275	-213	-488
4	32	7969	off		.98	.166	28.0	-1.4	-----	199.5	-394	-329	-723
5	1	7952	off		.96	.902	33.5	.6	-----	35.9	105	190	295
5	2	7952	off		.99	.764	33.5	.5	-----	43.7	81	153	234
5	3	7952	off		1.00	.549	33.5	.2	-----	61.4	22	107	129
5	4	7952	off		.98	.387	33.5	.1	-----	85.3	-2	72	70
5	5	7946	208	.00506	.96	.882	33.5	.4	-----	36.7	177	81	258
5	6	7940	271	.00537	1.00	.835	33.5	.2	-----	40.3	163	81	244
5	7	7934	270	.00404	.96	.633	33.5	.2	-----	51.0	125	51	176
5	8	7928	343	.00479	.95	.582	33.5	-.1	-----	54.9	105	31	136
5	9	7922	362	.00438	.98	.506	33.5	.0	-----	65.0	83	19	102
5	10	7916	438	.00460	.99	.463	33.5	.2	-----	71.8	67	-4	63
5	11	7910	373	.00332	.98	.378	33.5	.2	-----	86.8	37	-21	16
5	12	7904	437	.00361	.96	.343	33.5	.2	-----	93.9	22	-79	-57
5	13	7898	493	.00365	1.00	.318	33.5	-.3	-----	105.3	-12	-99	-111
5	14	7892	590	.00393	.99	.283	33.5	-.4	-----	117.0	-16	-132	-148
5	15	7886	645	.00398	1.00	.263	33.5	-.3	-----	127.1	-32	-167	-199
5	16	7880	714	.00398	.99	.236	33.5	-.3	-----	140.4	-50	-209	-259
5	17	7874	798	.00410	1.00	.218	33.8	-.3	-----	153.4	-56	-235	-291
5	18	7868	875	.00422	.98	.199	33.5	-.3	-----	163.8	-98	-284	-382
5	19	7862	965	.00431	.93	.176	33.5	-.4	-----	176.3	-145	-326	-471
5	20	7856	271	.00331	.98	.525	33.5	-.0	-----	62.1	102	41	143
5	21	7832	off		1.00	.476	33.5	.1	-----	69.7	55	93	148
5	22	7820	off		1.00	.371	33.5	-.2	-----	89.4	-12	72	60
5	23	7808	off		1.03	.280	33.5	-.2	-----	121.9	-67	19	-48
5	24	7796	off		1.00	.222	33.5	-.2	-----	148.7	-153	-69	-222
5	25	7784	off		.98	.143	33.5	-.1	-----	128.0	-112	-21	-133
5	26	7772	off		1.04	.133	33.5	-.1	-----	256.4	-296	-325	-621
13	1	8135	328	-------	.98	.980	29.7	-1.0	-0.6	34.4	169	21	190
13	2	8123	343	-------	1.05	.760	29.7	-1.1	-2.1	48.0	142	-31	111
13	3	8111	368	-------	1.05	.560	29.7	-1.2	-2.2	64.7	108	-92	16
13	4	8099	504	-------	1.05	.430	29.7	-.9	-3.3	84.9	85	-120	-35
13	5	8087	519	.00375	1.13	.370	29.7	-.5	-3.6	105.7	4	-136	-133
13	6	8075	640	.00388	1.05	.280	29.7	-.5	-4.0	127.9	-30	-221	-252
13	7	8063	790	.00404	1.05	.240	29.7	-.3	-4.3	150.0	-104	-282	-386
13	8	8051	1016	.00419	.98	.190	29.7	-.4	-4.6	178.9	-162	-380	-542
13	9	8039	1168	-------	1.05	----	29.7	-.5	-4.5	----	----	----	----
13	10	8027	1170	.00404	1.04	.170	29.7	-.5	-4.6	210.5	-207	-481	-688
13	11	8015	off		1.08	1.060	29.7	-2.2	6.3	34.7	132	114	246
13	12	8003	off		1.05	.730	29.7	-1.4	2.4	48.7	94	72	166
13	13	7991	off		1.05	.540	29.7	-1.2	.5	65.7	32	50	81
13	14	7979	off		.98	.400	29.7	-.9	-.8	83.5	-15	-3	-18
13	15	7967	off		.98	.310	29.7	-.8	-1.6	106.5	-78	-46	-124
13	16	7955	off		1.05	.280	29.7	-.7	-2.1	127.1	-81	-111	-193
13	17	7943	off		.98	.220	29.7	-.5	-2.5	153.2	-139	-194	-332
13	18	7931	off		.88	.160	29.7	-.5	-2.8	181.0	-199	-295	-493
13	19	7919	off		1.04	.150	29.7	-.4	-3.1	214.4	-298	-347	-645
19a	1	8136	388	-------	.99	.355	29.7	-.5	-.2	95.8	15	-91	-76
19a	2	8118	388	-------	2.08	.746	29.7	-1.2	2.7	95.8	265	71	337
19a	3	8100	367	-------	2.61	.961	29.7	-2.1	4.2	93.2	368	135	503
19a	4	8082	363	-------	2.89	1.066	29.7	-3.2	5.7	92.6	456	154	610
19a	5	8034	780	.00405	1.04	.235	29.7	-.7	-1.2	150.9	-78	-252	-330
19a	6	8016	780	.00410	2.26	.517	29.7	-1.6	.1	148.3	186	-68	118
19a	7	7998	776	.00403	2.54	.569	29.7	-2.1	.8	150.9	230	-33	197
19a	8	7980	773	.00412	2.92	.674	29.7	-3.7	-1.8	146.2	292	15	308
19a	9	7950	980	.00352	1.04	.157	29.7	-.8	-1.4	222.7	-240	-534	-774
19a	10	7932	976	.00347	2.24	.334	29.7	-1.5	-.2	224.8	----	----	----
19a	11	7914	968	.00334	2.40	.344	29.7	-1.7	-.2	233.1	----	----	----
19a	12	7896	960	.00336	3.31	.488	29.7	-3.4	.8	226.9	180	-134	46
19a	13	7878	956	.00333	2.68	.390	29.7	-3.0	.1	229.0	42	-208	-166
19b	1	8147	off		1.04	.386	29.7	-.9	2.4	92.6	-6	9	3
19b	2	8140	off		2.19	.878	29.7	-2.4	5.8	85.9	174	246	420
19b	3	8090	off		2.48	.953	29.7	-2.6	7.6	89.0	254	271	525
19b	4	8047	off		3.10	1.224	29.7	-4.3	9.1	86.4	341	394	735
19b	5	8016	off		.97	.232	29.7	-.5	.8	141.6	-145	-132	-277
19b	6	8009	off		2.29	.533	29.7	-1.6	3.2	145.7	101	101	203
19b	7	7990	off		2.65	.643	29.7	-1.8	4.2	139.5	192	136	329
19b	8	7982	off		3.20	.742	29.7	-2.0	4.8	145.7	204	224	428
19b	9	7975	off		1.04	.159	29.7	-.6	.4	220.7	-303	-313	-616
19b	10	----	off		2.52	----	29.7	----	2.2	----	----	----	----
19b	11	7919	off		2.52	.389	29.7	-1.7	-----	217.0	-32	-26	-58
19b	12	7912	off		2.93	.442	29.7	-1.9	-----	222.2	16	26	42
19b	13	7904	off		2.95	.462	29.7	-1.9	-----	213.4	0	81	81

[a]No values of torque coefficient were obtained for power-off condition.

NATIONAL ADVISORY
COMMITTEE FOR AERONAUTICS

TABLE II

MANEUVERING-FLIGHT MEASUREMENTS

Flight	Run	Time (sec)	Altitude (ft)	q_c	V_e (mph)	$n_{c.g.}$ (g)	n_t (g)	δ_e (deg)	F_e (lb)	$\dot{\theta}$ (radians/sec)	ζ (deg)	β (deg)	C_L
14	[a]1	0.50	25100	0.00768	126	0.98	0.98	-0.6	-4.0	0	-0.8	-----	0.823
		.70			126	.89	.32	-19.3	-39.0	.050	-.9		
		1.30			124	1.78	2.26	-17.0	-27.5	.590	-----		
		1.60			123	1.42	2.07	-13.1	-----	.295	-----		
14	[a]2	1.00	25200	.00718	156	.98	.98	-.8	-1.3	.002	-2.4	-----	.529
		1.15			156	1.05	.00	-12.7	-63.0	.140	-2.3		
		1.70			156	2.85	3.06	-12.3	-38.0	.690	-----		
		1.90			151	2.40	3.00	-9.4	-3.0	.555	-----		
14	[a]3	2.30	25250	.00542	184	1.07	.98	-.8	-2.4	0	-2.6	-----	.416
		2.45			184	1.05	-.24	-10.8	-77.8	.095	-2.1		
		3.10			179	3.71	4.07	-9.4	-----	.620	-----		
		3.20			176	3.00	3.90	-9.2	-----	.365	-----		
14	[a]4	.50	25000	off	111	.98	.98	-1.8	-1.9	0	6.1	-----	1.033
		1.00			111	.88	.45	-20.6	-35.0	.050	6.0		
		1.70			116	1.82	1.97	-16.6	-----	.490	-----		
		2.00			115	1.01	1.90	-15.8	-----	.205	-----		
14	[a]5	.60	24900	off	158	1.00	.95	-1.0	-9.6	0	1.1	-----	.529
		.80			158	.94	.22	-18.6	-65.5	.100	1.2		
		1.30			158	2.98	2.81	-16.0	-47.0	.735	-----		
		1.62			153	2.40	3.00	-12.7	-----	.325	-----		
14	[a]6	.80	24400	off	182	.98	.98	-.4	-6.3	0	0	-----	.390
		1.00			182	1.05	.00	-12.7	-73.0	.085	0		
		1.55			178	3.62	3.70	-13.7	-49.0	.780	-----		
		1.80			177	2.93	3.86	-12.3	-----	.325	-----		
15	1	.60	9000	.00343	188	1.07	.98	-1.0	-16.5	.015	-1.8	-----	.408
		.80			188	1.23	.20	-13.1	-71.8	.205	.8		
		1.40			188	3.26	3.77	-10.8	12.0	.300	7.3		
		1.60			187	3.18	3.68	-9.2	22.5	.110	6.8		
15	[a]2	.90	9000	.00367	186	.98	.98	-1.0	.3	0	-1.5	-----	.385
		1.14			186	1.02	.05	-14.3	-50.8	.150	-.3		
		1.71			185	3.91	4.08	1.3	-----	.490	-----		
		1.71			185	3.91	4.08	1.3	-----	.490	-----		
15	5	.30	9000	off	184	.98	.98	-1.0	0	0	1.4	-----	.389
		.625			184	1.05	.10	-15.7	-69.0	.090	2.8		
		1.20			184	3.58	4.23	2.3	30.0	.340	15.6		
		1.15			184	3.58	4.19	1.7	21.0	.395	14.8		
15	[a]6	.70	9000	off	183	1.11	.98	-1.0	-1.0	0	1.6	-----	.448
		.96			183	1.02	.19	-16.6	-80.0	.240	2.8		
		1.60			183	3.86	4.35	2.3	35.5	.360	18.8		
		1.44			183	3.68	4.35	.3	-8.0	.600	16.8		
16a	1	-.40	7020	.00336	211	1.09	1.02	-1.0	-----	0	-1.5	-----	.331
		-.20			211	1.10	.32	-8.8	-----	.125	-1.1		
		.45			211	4.38	4.75	-.9	-----	.330	6.9		
		.375			211	4.11	4.74	-.6	-----	.405	6.4		
16a	2	.20	7000	.00332	213	1.11	.98	-1.0	-----	0	-1.5	-----	.330
		.40			213	1.06	.10	-13.7	-----	.105	-1.1		
		1.00			213	4.91	5.64	2.5	-----	.475	10.1		
		.975			213	4.60	5.61	1.3	-----	.505	11.1		
16a	[a]3	.40	6970	.00343	209	1.04	1.01	-1.0	-----	.010	-1.6	-----	.337
		.70			209	1.05	.32	-11.0	-----	.230	-.9		
		1.25			209	5.11	6.08	1.5	-----	.600	13.0		
		1.28			209	5.20	6.08	2.2	-----	.550	13.0		
16a	4	-.30	6800	.00412	232	1.16	.98	-1.0	-----	0	-2.1	-----	.288
		-.08			232	1.12	-.07	-10.4	-----	.170	-1.2		
		.50			232	5.56	6.03	.5	-----	.460	8.7		
		.50			232	5.56	6.03	.5	-----	.460	8.7		
17a	1	1.00	8500	.00414	241	1.07	1.06	-1.0	7.6	0	-1.9	-----	.247
		1.30			241	1.09	.76	-4.5	-33.0	.010	-1.1		
		2.10			239	4.53	4.56	-.2	-22.5	.250	4.4		
		2.15			238	4.54	4.43	-.4	-24.5	.210	4.3		
17a	2	.70	8670	.00415	241	1.07	.98	-1.0	8.5	0	-1.9	-----	.246
		1.20			241	1.21	.79	-5.3	-36.0	.090	-1.5		
		2.23			236	5.65	5.68	.2	39.0	.270	3.0		
		2.20			236	5.37	5.84	.2	37.5	.290	-----		

[a]Stall pull-up

NATIONAL ADVISORY
COMMITTEE FOR AERONAUTICS

TABLE II.- MANEUVERING-FLIGHT MEASUREMENTS - Continued

Tail loads (lb)									$\ddot{\theta}_{max}$ (radians/sec^2)	$\dot{\delta}_e$ (deg/sec)	c.g. (percent M.A.C)	Flight	Run
Elevator			Stabilizer			Total							
Left	Right	Total	Left	Right	Total	Left	Right	Total					
12.1	9.9	22.0	150.8	34.5	185.3	165.1	38.8	203.0	1.17	168.0	29.7	14	1
-185.0	-175.0	-360.1	-60.1	-200.4	-260.5	-245.5	-375.6	-620.6					
-55.0	-100.0	-155.0	320.0	200.0	520.0	260.0	85.0	355.0					
30.2	27.8	58.0	555.7	478.0	1033.7	562.4	495.0	1057.0					
-2.2	0	-2.2	106.3	-38.8	67.4	110.1	-38.3	71.0	2.50	162.0	29.7	14	2
-278.4	-255.7	-534.1	-225.5	-393.8	-619.4	-497.7	-652.8	-1150.0					
-61.5	-144.3	-205.8	606.4	341.0	947.4	543.8	193.1	737.0					
59.9	3.2	63.1	836.2	685.2	1521.4	871.8	674.4	1546.0					
-13.5	-12.4	-25.9	66.9	-105.2	-38.3	54.0	-121.4	-67.0	2.38	117.6	29.7	14	3
-366.3	-334.0	-700.3	-233.1	-420.0	-653.1	-577.3	-783.4	-1360.0					
9.7	-82.5	-72.8	919.3	611.8	1531.1	947.4	519.0	1466.0					
20.2	.3	20.5	1056.3	751.0	1807.3	1066.1	910.7	1976.0					
15.0	0	15.0	90.0	125.0	215.0	105.0	125.0	230.0	1.27	176.0	29.7	14	4
-130.6	-142.7	-273.3	-87.4	-70.3	-157.7	-216.1	-213.4	-429.0					
-39.9	-37.0	-76.9	236.8	832.5	469.4	197.5	266.5	464.0					
-16.2	4.5	-11.7	522.8	403.6	926.3	499.0	408.4	907.0					
-4.1	1.4	-2.6	75.0	27.5	102.5	69.9	21.7	91.0	1.83	148.0	29.7	14	5
-218.0	-241.0	-459.0	-232.0	-251.0	-482.0	-448.0	-485.0	-933.0					
-116.5	-127.9	-244.4	413.3	271.4	684.6	293.5	191.0	484.0					
15.0	-5.0	10.0	850.0	730.0	1580.0	865.0	725.0	1590.0					
-3.9	.3	-3.6	0	0	0	-2.2	-5.7	-7.0	2.04	160.0	29.7	14	6
-270.0	-286.0	-556.0	-308.0	-325.0	-633.0	-562.0	-605.0	-1168.0					
-120.0	-155.0	-275.0	545.0	525.0	1070.0	425.0	370.0	795.0					
-28.0	-19.0	-48.0	828.0	750.0	1578.0	790.0	719.0	1508.0					
0.0	-20.0	-20.0	20.0	-60.0	-40.0	20.0	-80.0	-60.0	2.19	80.0	29.7	15	1
-305.0	-355.0	-660.0	-205.0	-320.0	-525.0	-510.0	-675.0	-1185.0					
87.4	76.9	164.3	699.2	488.8	1188.0	785.5	558.9	1344.0					
136.5	126.8	263.3	681.9	451.0	1133.0	845.9	573.0	1418.0					
-2.2	-13.0	-15.1	41.3	-80.9	-39.7	40.2	-96.6	-56.0	2.63	108.0	29.7	15	2
-350.0	-350.0	-700.0	-260.0	-395.0	-655.0	-610.0	-745.0	-1355.0					
150.0	150.0	300.0	675.0	900.0	1575.0	825.0	1050.0	1875.0					
150.0	150.0	300.0	675.0	900.0	1575.0	825.0	1050.0	1875.0					
-9.4	-7.8	-16.0	-1.0	-13.0	-14.5	-10.1	-20.8	-30.0	2.16	--------	29.7	15	5
-340.0	-345.0	-685.0	-290.0	-315.0	-605.0	-630.0	-660.0	-1290.0					
155.7	151.1	306.8	774.7	755.3	1530.0	912.8	875.1	1787.0					
145.0	145.0	290.0	815.0	775.0	1590.0	960,0	920.0	1880.0					
-10.8	9.4	-1.4	13.0	23.5	36.4	2.2	32.9	35.0	2.47	--------	29.7	15	6
-285.0	-345.0	-630.0	-265.0	-270.0	-535.0	-550.0	-615.0	-1165.0					
144.1	154.9	298.9	833.0	830.8	1663.8	977.1	984.9	1961.0					
170.0	170.0	340.0	920.0	925.0	1845.0	1090.0	1095.0	2185.0					
-24.3	-28.1	-52.3	0	-177.0	-177.0	-22.1	-203.4	-225.0	1.75	64.0	29.7	16a	1
-308.6	-314.0	-622.6	-191.0	-372.0	-563.8	-496.3	-679.8	-1176.0					
180.0	160.0	340.0	915.0	555.0	1475.0	1100.0	710.0	1805.0					
195.0	175.0	370.0	955.0	610.0	1565.0	1150.0	785.0	1935					
-12.7	-16.2	-28.9	-3.2	-158.3	-161.6	-5.4	-180.2	-185.0	2.60	92.0	29.7	16a	2
-365.8	-362.5	-728.3	-309.1	-438.6	-747.8	-692.7	-788.8	-1481.0					
246.8	261.4	508.2	1197.7	907.4	2105.1	1480.9	1154.5	2635.0					
235.0	240.0	475.0	1210.0	930.0	2140.0	1445.0	1170.0	2615.0					
-13.0	-17.5	-30.5	8.1	-169.4	-161.3	0	-195.3	-195.0	2.33	72.0	29.7	16a	3
-389.5	-414.3	-803.9	-252.0	-427.3	-679.2	-639.9	-838.4	-1478.0					
220.0	280.0	500.0	1280.0	1040.0	2320.0	1560.0	1260.0	2820.0					
240.0	290.0	530.0	1270.9	995.0	2265.0	1510.0	1285.0	2795.0					
-15.1	-20.8	-35.9	-49.1	-239.0	-288.0	-62.0	-263.3	-325.0	2.47	80.0	29.7	16a	4
-440.0	-400.0	-840.0	-380.0	-515.0	-895,0	-820.0	-915.0	-1735.0					
237.4	220.7	458.0	1326.1	888.0	2214.1	1563.8	1108.7	2671.0					
237.4	220.7	458.0	1326.1	888.0	2214.1	1563.8	1108.7	2671.0					
-26.9	-3.5	-30.3	-23.2	-210.4	-233.6	-45.9	-224.4	-270.0	.77	24.0	29.7	17a	1
-214.7	-181.3	-396.0	-116.5	-309.7	-426.2	-334.5	-489.9	-824.0					
120.0	120.0	240.0	855.0	460.0	1315.0	975.0	580.0	1555.0					
140.0	120.0	260.0	850.0	440.0	1290.0	990.0	560.0	1550.0					
-30.0	-15.0	-45.0	-30.0	-240.0	-270.0	-60.0	-255.0	-315	.90	22.4	29.7	17a	2
-230.4	-206.1	-436.5	-88.5	-302.1	-390.6	-318.7	-508.7	-826.0					
190.0	190.0	380.0	1170.0	745.0	1915.0	1360.0	935.0	2295.0					
189.4	188.3	377.7	1186.9	771.5	1958.4	1375.4	960.7	2335.0					

NATIONAL ADVISORY
COMMITTEE FOR AERONAUTICS

TABLE II.- MANEUVERING FLIGHT MEASUREMENTS - Continued

Flight	Run	Time (sec)	Altitude (ft)	q_c	V_c (mph)	$n_{c.g.}$ (g)	n_t (g)	δ_e (deg)	F_e (lb)	$\dot{\theta}$ (radians/sec)	ζ (deg)	β (deg)	C_L
17a	3	1.80	8670	0.00415	241	1.09	1.02	-1.0	7.0	0	-1.9	-----	0.249
		2.20			241	1.26	.93	-6.1	-40.5	.150	-1.3		
		2.90			239	4.90	4.95	-2.6	-6.0	.380	6.0		
		3.80			239	4.71	4.98	.9	7.0	.440	5.8		
18	1	.80	7800	.00349	160	1.07	.98	-1.6	-1.5	0	1.1	-----	.560
		1.00			161	1.05	.69	-3.7	-20.5	.000	1.1		
		3.05			155	2.47	2.56	-1.6	15.8	.145	7.4		
		3.10			154	2.43	2.56	-.2	17.5	.123	7.2		
18	[a]2	.70	7700	.00345	163	1.07	.98	-1.6	-7.5	0	.9	-----	.544
		.90			163	.91	.61	-8.0	-28.0	.085	.9		
		2.30			158	3.13	3.06	-5.7	17.0	.350	13.0		
		2.50			157	2.78	3.19	-2.2	19.4	.215	12.3		
18	3	-.20	7900	.00350	161	1.08	.95	-1.4	-17.0	0	1.1	-----	.563
		-.10			161	.88	.75	-5.9	-13.5	.033	1.3		
		1.70			156	2.32	2.26	-3.5	-6.0	.177	7.2		
		3.00			146	2.01	2.12	1.7	22.5	.055	6.4		
20	1	1.60	7000	.00341	293	1.17	1.10	-1.2	-7.0	.009	-1.2	-----	.184
		1.80			293	1.37	1.20	-2.6	-27.0	.060	-1.1		
		2.80			289	4.95	5.10	-.8	2.0	.255	3.1		
		2.80			289	4.95	5.10	-.8	2.0	.255	3.1		
20	2	1.20	7000	.00341	289	1.10	1.10	-1.0	-2.0	0	-1.3	-----	.183
		1.50			288	1.34	.98	-2.8	-38.0	.090	-.1		
		2.25			286	5.65	6.14	-.2	14.0	.350	4.4		
		2.30			286	5.69	6.08	-1.9	15.0	.275	4.6		
20	3	1.80	7000	.00333	297	1.12	1.06	-1.2	-3.5	0	-1.3	-----	.171
		2.00			297	1.24	1.12	-1.6	-11.0	.015	-1.2		
		3.85			287	5.18	5.30	-1.6	-5.0	.245	3.7		
		3.95			286	5.11	5.10	-.6	5.5	.190	3.3		
20	4	.90	7000	.00341	293	1.12	1.06	-1.2	-----	-.015	-1.5	-----	.176
		1.20			293	1.11	.98	-2.2	-17.0	.010	-1.3		
		2.50			287	5.47	5.50	.9	4.0	.275	4.2		
		2.50			287	5.47	5.50	.9	4.0	.275	4.2		
20	5	1.30	7000	Off	290	1.14	1.08	-1.0	-.8	-.003	.1	-----	.182
		1.50			290	1.15	1.00	-1.2	-10.0	.003	.1		
		3.10			285	4.20	5.11	-.6	-24.5	.330	5.7		
		3.30			283	5.01	5.32	-.2	-1.2	.290	5.7		
20	6	1.10	6000	Off	290	1.01	1.07	-1.0	-5.0	-.008	-.2	-----	.160
		1.60			290	1.62	1.22	-3.2	-37.5	.110	.2		
		2.55			285	4.97	5.40	-.2	-5.0	.285	4.9		
		2.60			284	4.95	5.38	.7	-25.0	.240	4.9		
20	7	1.30	7500	Off	285	1.09	1.05	-.8	-10.0	-.004	-.2	-----	.158
		1.50			285	1.44	.78	-4.2	-36.7	.090	.4		
		2.20			284	5.53	6.06	1.1	11.0	.245	6.6		
		2.10			284	5.56	6.19	.9	5.0	.390	6.6		
20	8	1.50	7500	Off	287	1.11	1.05	-1.0	-4.0	.003	-.1	-----	.181
		1.80			286	1.13	1.07	-1.4	-14.0	.010	.1		
		4.00			274	4.90	4.99	-1.2	-25.0	.295	6.1		
		4.70			260	4.53	4.59	-1.6	-4.0	.195	4.9		
21a	1	Steady	8500	.00407	240	1.00	.98	-.3	-----	0	-.3	1.1	.234
21a	2	1.10	8500	.00347	260	1.10	1.12	-2.3	-----	.020	.1	-6.5	.217
		1.40			260	1.27	1.06	-4.6	-----	.105	.4		
		2.03			258	3.92	4.13	-2.9	-----	.320	3.9		
		2.10			258	3.69	4.45	-1.7	-----	.260	3.9		
21a	3	.90	8000	.00375	252	1.00	.98	-1.9	-19.0	.035	0	-5.0	.215
		1.10			252	1.05	.90	-4.9	-44.0	.095	.8		
		1.90			250	5.11	4.85	-.8	1.0	.325	6.1		
		1.80			251	4.30	4.85	-1.9	-3.8	.400	5.8		
21a	4	.60	8900	.00455	227	.84	.90	-.8	-.6	.010	2.4	8.0	.219
		1.10			227	1.03	.93	-----	-40.5	.090	3.2		
		1.95			223	4.02	4.50	-2.6	19.0	.310	10.4		
		2.00			222	3.90	4.41	-2.7	18.2	.270	10.4		

[a]Stall pull-up.

NATIONAL ADVISORY
COMMITTEE FOR AERONAUTICS

TABLE II.- MANEUVERING FLIGHT MEASUREMENTS - Continued

Tail loads (lb)									$\ddot{\theta}_{max}$ (radians/sec^2)	$\dot{\delta}_a$ (deg/sec)	c.g. (percent M.A.C.)	Flight	Run
Elevator			Stabilizer			Total							
Left	Right	Total	Left	Right	Total	Left	Right	Total					
-37.8	-28.6	-66.4	-32.9	-220.1	-253.0	-69.6	-248.4	-318.0	0.88	22.0	29.7	17a	3
-265.4	-236.3	-501.7	-84.2	-282.7	-366.9	-350.7	-516.6	-867.2					
60.0	60.0	120.0	920.0	550.0	1470.0	980.0	610.0	1590.0					
83.6	93.3	177.0	917.2	555.7	1472.8	1000.0	648.4	1648.4					
-15.7	-4.4	-20.1	80.7	-9.4	71.2	66.1	-13.0	53.1	.69	56.0	29.7	18	1
-112.8	-95.8	-208.5	-23.7	-85.2	-109.0	-135.4	-181.0	-316.4					
70.0	60.0	130.0	470.0	275.0	750.0	540.0	335.0	875.0					
80.4	69.1	149.5	492.0	279.5	771.5	572.5	348.4	920.9					
-11.1	-8.1	-19.2	97.7	-29.1	68.5	86.3	-36.2	50.2	.90	80.0	29.7	18	2
-165.6	-181.3	-346.9	-38.8	-155.4	-194.2	-203.0	-336.0	-539.0					
35.0	0	35.0	660.0	365.0	1045.0	695.0	385.0	1080.0					
108.5	112.8	221.2	667.9	444.6	1112.5	775.3	556.0	1331.3					
-40.5	-34.2	-74.7	47.2	-48.6	-1.4	6.2	-82.2	-75.0	.49	51.0	29.7	18	3
-110.6	-111.1	-221.7	1.4	-107.1	-105.7	-111.1	-215.3	-326.4					
-5.0	-20.0	-25.0	395.0	290.0	585.0	390.0	270.0	560.0					
84.7	92.0	176.7	400.3	252.0	652.3	485.6	344.7	829.3					
-75.0	-45.0	-120.0	-155.0	-435.0	-590.0	-230.0	-480.0	-710.0	.52	10.0	29.7	20	1
-158.1	-134.9	-293.0	-132.7	-408.9	-541.7	-290.0	-542.3	-832.3					
111.4	133.0	244.4	810.3	349.6	1159.9	921.3	482.3	1503.5					
111.4	133.0	244.4	810.3	349.6	1159.9	921.3	482.3	1503.5					
-55.0	-46.4	-101.5	-175.9	-445.0	-620.4	-230.1	-491.4	-721.5	.90	17.6	29.7	20	2
-216.3	-209.9	-426.2	-219.0	-466.1	-685.2	-435.6	-655.7	-1090.3					
180.0	200.0	380.0	1060.0	575.0	1635.0	1080.0	770.0	1910.0					
214.2	219.0	433.2	1098.4	542.7	1641.2	1186.9	768.8	1955.7					
-42.9	-24.0	-66.9	-195.3	-449.9	-645.2	-237.4	-474.2	-711.5	.25	4.0	29.7	20	3
-87.4	-70.7	-158.1	-185.6	-426.7	-611.8	-272.9	-496.6	-668.4					
70.0	35.0	105.0	820.0	335.0	1155.0	890.0	370.0	1260.0					
105.0	70.0	175.0	780.0	295.0	1075.0	885.0	365.0	1240.0					
-50.0	-30.0	-80.0	-210.0	-450.0	-660.0	-260.0	-480.0	-740.0	.47	5.2	29.7	20	4
-118.4	-83.4	-201.8	-220.1	-460.7	-680.9	-338.4	-542.7	-880.2					
103.6	113.0	216.6	962.5	382.0	1344.4	1065.0	495.0	1560.0					
103.6	113.0	216.6	962.5	382.0	1344.4	1065.0	495.0	1560.0					
-51.0	-28.0	-79.0	-265.0	-283.0	-548.0	-316.0	-311.0	-627.0	.36	6.0	29.7	20	5
-85.0	-79.0	-164.0	-280.0	-317.0	-597.0	-365.0	-396.0	-761.0					
-7.5	12.5	5.0	618.0	626.0	1244.0	610.0	645.0	1255.0					
106.0	111.0	217.0	610.0	711.0	1321.0	716.0	822.0	1539.0					
-61.0	-36.0	-97.0	-265.0	-304.0	-569.0	-326.0	-340.0	-666.0	.63	10.8	29.7	20	6
-211.0	-187.0	-398.0	-210.0	-228.0	-438.0	-421.0	-415.0	-836.0					
92.5	102.0	194.5	767.0	636.5	1403.5	865.0	725.0	1590.0					
97.0	111.0	208.0	750.0	635.0	1385.0	847.0	746.0	1593.0					
-106.0	-44.0	-150.0	-266.0	-318.0	-584.0	-372.0	-362.0	-734.0	1.18	25.6	29.7	20	7
-335.0	-265.0	-600.0	-310.0	-351.0	-661.0	-645.0	-616.0	-1261.0					
148.0	235.0	383.0	910.0	743.0	1653.0	1058.0	978.0	2036.0					
100.0	163.0	265.0	1045.0	766.0	1811.0	1145.0	934.0	2079.0					
41.0	-21.0	20.0	-265.0	-297.0	-562.0	-224.0	-318.0	-542.0	.30	2.4	29.7	20	8
-93.0	-75.0	-168.0	-250.0	-297.0	-547.0	-343.0	-372.0	-715.0					
0	-18.0	-18.0	665.0	621.0	1286.0	665.0	603.0	1268.0					
106.0	83.0	189.0	559.0	697.0	1256.0	665.0	780.0	1445.0					
-26.4	-3.5	-29.9	-57.2	-242.8	-300.0	-83.6	-243.9	-327.5			30.6	21a	1
-115.0	-65.0	-180.0	70.0	-350.0	-280.0	-45.0	-415.0	-460.0	.69	22.0	30.6	21a	2
-257.9	-199.6	-457.5	10.8	-397.1	-282.0	-247.4	-596.9	-843.3					
-5.0	-5.0	-10.0	775.0	225.0	1010.0	770.0	220.0	990.0					
25.4	38.3	63.7	831.9	259.0	1090.9	856.8	297.0	1153.9					
-160.0	-130.0	-290.0	-5.0	-365.0	-370.0	-165.0	-495.0	-660.0	.77	21.6	30.6	21a	3
-264.4	-214.2	-478.5	-47.5	-406.8	-454.3	-311.4	-620.0	-931.4					
70.0	70.0	140.0	980.0	360.0	1340.0	1050.0	410.0	1460.0					
53.4	38.3	91.7	974.3	383.1	1357.4	1027.3	421.7	1448.1					
-65.0	-45.0	-110.0	-275.0	-75.0	-350.0	-340.0	-120.0	-460.0	.77	17.2	30.6	21a	4
-193.1	-164.0	-357.2	-293.5	-88.5	-382.0	-470.4	-249.3	-719.7					
110.0	100.0	210.0	580.0	730.0	1320.0	645.0	880.0	1520.0					
133.5	113.8	246.3	597.8	738.0	1335.8	673.3	898.8	1572.1					

NATIONAL ADVISORY
COMMITTEE FOR AERONAUTICS

TABLE II.- MANEUVERING-FLIGHT MEASUREMENTS - Continued

Flight	Run	Time (sec)	Altitude (ft)	q_c	V_e (mph)	$n_{c.g.}$ (g)	n_t (g)	δ_e (deg)	F_e (lb)	$\dot{\theta}$ (radians/sec)	ζ (deg)	β (deg)	C_L
21a	5	1.10 1.375 2.10 2.00	9000	0.00423	236 236 223 224	.99 1.17 4.46 4.27	1.02 .63 4.91 4.91	-0.5 -6.2 .7 -.5	-1.4 -48.0 15.3 10.0	.015 .120 .320 .410	.3 .4 6.8 6.6	4.5	0.239
21a	6	Steady	7500	.00394	263	1.00	.98	0	-.1	.018	-.6	1.3	.195
21a	7	.20 .40 1.15 1.10	7500	.00362	275 275 274 274	.88 1.04 3.78 3.76	1.06 .88 4.75 4.45	-1.2 -2.7 .3 -.8	-17.1 -32.5 -2.0 2.0	.020 .055 .185 .240	0 .1 3.4 3.5	-5.0	.157
21a	8	1.50 1.70 2.50 2.50	7500	.00390	263 263 262 262	1.00 1.04 4.00 4.00	1.00 .80 4.39 4.39	-.6 -2.3 -.3 -.3	-9.5 -34.1 -2.2 -2.2	.018 .035 .325 .325	.1 .3 4.4 4.4	-3.0	.193
21a	9	1.00 1.20 2.05 2.00	7500	.00403	259 259 256 257	1.00 1.06 4.67 4.10	.98 .84 4.69 4.71	-.5 -2.6 .5 -.3	-6.4 -28.0 9.0 9.0	.022 .070 .270 .315	.1 .1 6.6 6.7	6.0	.198
21a	10	1.30 1.60 2.40 2.40	7500	.00400	259 259 256 256	1.00 1.20 4.08 4.08	1.00 .90 4.51 4.51	-.9 -4.0 .0 0	-8.0 -34.0 -2.5 -2.5	.020 .090 .265 .265	.1 .6 4.3 4.3	4.9	.197
21b	1	Steady	7500	.00334	300	1.11	.90	-.5	------	.040	-2.0	1.4	.158
21b	2	-.10 .10 .80 .80	7300	.00333	288 288 287 287	1.02 1.06 3.75 3.75	.93 1.06 3.95 3.95	-2.3 -3.7 -.9 -.9	------ ------ ------ ------	.025 .070 .060 .060	-3.1 -1.7 .9 .9	-4.0	.156
21b	3	1.50 1.80 2.60 2.60	--------	--------	296 296 294 294	1.01 1.23 3.87 3.87	.98 .98 4.18 4.18	-1.7 -3.3 -.8 -.8	-6.0 -34.0 2.5 2.5	.000 .075 .230 .230	-2.0 -1.8 1.2 1.2	-1.2	.155
21b	4	Steady	9000	.00325	301	1.00	1.00	-.6	------	0	-2.0	1.5	.150
21b	5	.80 1.10 2.10 2.10	8500	.00324	281 281 279 279	1.18 1.19 4.56 4.56	.92 .90 4.69 4.69	-1.8 -3.7 -1.8 -1.8	-1.2 -33.0 14.0 14.0	-.005 .065 .195 .195	-1.7 -1.6 1.7 1.7	5.2	.159
21b	6	.70 1.10 1.85 1.80	8500	.00353	---- ---- ---- ----	1.02 1.12 4.23 4.14	.93 .90 4.45 4.51	-.8 -2.9 -.5 -1.0	------ -33.5 4.0 4.0	0 .075 .212 .257	-1.9 -1.5 1.5 1.6	3.7	.157
22a	1	Steady	6500	Off	236	1.18	1.15	-.3	------	-.015	1.9	2.9	.284
22a	2	-.10 .15 .90 .83	4500	Off	254 253 249 250	1.14 1.33 4.22 4.18	1.15 .93 4.79 4.81	-1.7 -5.1 -.6 -1.9	-14.2 2.5 3.0 1.0	-.005 .100 .200 .280	.2 1.5 6.1 6.6	-4.4	.239
22a	3	-.20 .10 .90 .85	6500	Off	241 241 238 238	1.00 1.06 4.34 4.30	1.06 .72 4.79 4.75	-.8 ------ -.8 -1.4	-7.5 -45.5 1.0 .5	-.005 .040 .280 .320	.4 .8 8.8 ----	-2.4	.235
22a	4	1.10 1.37 2.35 2.40	7000	Off	227 227 224 224	1.01 1.21 3.98 3.94	.98 .90 4.34 4.31	-2.1 -6.0 -4.6 -3.7	-10.5 -39.5 -11.0 -8.0	0 .080 .325 .295	.3 .9 12.2 ----	9.9	.266
22a	5	.50 .83 1.64 1.64	7000	Off	232 231 229 229	.95 1.30 4.65 4.65	1.02 .90 5.10 5.10	-1.0 -5.5 -.5 -.5	-5.0 -41.5 7.5 7.5	0 .095 .410 .410	2.1 3.2 11.3 11.3	6.9	.239
22c	1	Steady	8000	Off	290	.97	1.06	.2	2.0	0	-1.6	1.7	.155

NATIONAL ADVISORY
COMMITTEE FOR AERONAUTICS

TABLE II.- MANEUVERING-FLIGHT MEASUREMENTS - Continued

Tail load (lb)									$\ddot{\theta}_{max}$ (radians/sec²)	$\dot{\delta}_e$ (deg/sec)	c.g. (percent M.A.C.)	Flight	Run
Elevator			Stabilizer			Total							
Left	Right	Total	Left	Right	Total	Left	Right	Total					
-34.3	-1.4	-35.6	-139.2	-151.1	-290.3	-173.0	-152.0	-325.0	1.23	46.8	30.6	21a	5
-240.0	-220.0	-460.0	-240.0	-260.0	-495.0	-480.0	-480.0	-960.0					
127.9	124.6	252.5	749.9	665.7	1415.7	876.0	789.0	1665.0					
122.5	113.8	236.3	798.5	677.6	1476.1	920.0	790.0	1710.0					
-10.8	12.4	2.6	-123.6	-335.0	-458.1	-133.0	-323.0	-456.0			30.6	21a	6
-125.7	-74.5	-200.2	0.	-452.1	-452.1	-125.0	-526.0	-651.0	.74	28.0	30.6	21a	7
-260.6	-172.1	-432.7	-65.8	-498.5	-564.3	-325.0	-670.0	-995.0					
90.0	80.0	170.0	830.0	175.0	1005.0	920.0	255.0	1175.0					
80.9	69.1	150.0	863.2	189.9	1053.1	945.0	246.0	1191.0					
-80.0	-40.0	-120.0	-25.0	-385.0	-410.0	-105.0	-425.0	-530.0	.60	20.0	30.6	21a	8
-168.3	-126.2	-294.6	-55.0	-445.6	-500.7	-222.0	-571.0	-793.0					
70.7	79.0	149.7	824.4	273.0	1097.3	894.0	352.0	1246.0					
70.7	79.0	149.7	824.4	273.0	1097.3	894.0	352.0	1246.0					
-66.4	-38.0	-104.4	-278.4	-178.0	-456.4	-344.0	-226.0	-570.0	.74	19.6	30.6	21a	9
-202.2	-178.6	-378.7	-318.3	-239.5	-557.8	-320.0	-417.0	-937.0					
100.0	110.0	215.0	510.0	615.0	1130.0	610.0	725.0	1335.0					
98.2	101.4	199.6	522.2	636.6	1158.9	-620.0	737.0	1357.0					
-45.6	-22.7	-68.3	-246.0	-219.0	-465.1	-291.0	-241.0	-532.0	.74	15.2	30.6	21a	10
-191.0	-159.7	-350.7	-271.9	-246.0	-517.9	-462.0	-405.0	-867.0					
100.6	102.5	203.1	536.3	570.8	1107.1	638.0	672.0	1311.0					
100.6	102.5	203.1	536.3	570.8	1107.1	638.0	672.0	1311.0					
-39.2	0.3	-39.9	-230.4	-413.3	-643.6	-269.0	-413.0	-682.0			30.6	21b	1
-110.0	-70.0	-180.0	-80.0	-565.0	-645.0	-190.0	-635.0	-825.0	.76	15.2	30.6	21b	2
-239.0	-184.5	-423.5	-129.5	-580.7	-710.0	-368.0	-764.0	-1122.0					
62.6	84.7	147.3	670.1	82.0	752.1	732.0	166.0	898.0					
62.6	84.7	147.3	670.1	82.0	752.1	732.0	166.0	898.0					
-82.5	-22.1	-104.7	-124.1	-483.4	-607.5	-205.0	-505.0	-710.0	.52	10.8	30.6	21b	3
-205.0	-127.3	-332.3	-113.3	-453.2	-566.5	-318.0	-580.0	-898.0					
62.6	93.3	155.9	721.9	169.4	891.3	783.0	262.0	1045.0					
62.6	93.3	155.9	721.9	169.4	891.3	783.0	262.0	1045.0					
-42.9	4.6	-38.3	-217.4	-440.2	-657.7	-259.0	-436.0	-695.0			30.6	21b	4
-34.5	-31.3	-65.8	-372.3	-296.7	-669.0	-406.0	-327.0	-733.0	.60	16.0	30.6	21b	5
-198.5	-186.1	-384.7	-410.0	-321.0	-731.0	-610.0	-503.0	-1114.0					
155.4	156.5	311.8	472.1	609.6	1081.7	627.0	765.0	1392.0					
155.4	156.5	311.8	472.1	609.6	1081.7	627.0	765.0	1392.0					
-39.9	-7.0	-46.9	-304.3	-353.9	-658.2	-343.0	-360.0	-703.0	.64	---------	30.6	21b	6
-207.7	-160.8	-368.5	-334.5	-390.6	-725.1	-541.0	-340.0	-1081.0					
80.0	125.0	205.0	465.0	460.0	930.0	545.0	585.0	1130.0					
71.2	109.5	180.7	479.1	476.9	956.0	550.0	585.0	1135.0					
-16.0	3.1	-12.8	-91.5	-71.5	-162.9	-107.0	-68.0	-175.0			30.6	22a	1
-96.8	-70.7	-167.5	44.2	-320.5	-276.2	-52.0	-390.0	-442.0	1.10	---------	30.6	22a	2
-240.0	-180.0	-415.0	0.	-360.0	-360.0	-240.0	-540.0	-780.0					
55.8	81.5	137.3	926.9	289.2	1216.0	981.0	370.0	1351.0					
55.0	80.0	135.0	955.0	320.0	1275.0	1010.0	400.0	1410.0					
-55.0	-40.0	-100.0	10.0	-245.0	-235.0	-45.0	-285.0	-330.0	1.01	---------	30.6	22a	3
-200.2	-182.4	-382.5	-73.4	-328.0	-401.4	-271.0	-510.0	-782.0					
75.0	69.9	144.9	925.8	364.7	1290.5	1000.0	433.0	1433.0					
70.0	60.0	135.0	930.0	380.0	1310.0	1000.0	440.0	1440.0					
-77.7	-68.5	-146.0	-144.6	51.8	-92.0	-221.0	-17.0	-236.0	.74	---------	30.6	22a	4
-200.0	-195.0	-395.0	-225.0	-10.0	-235.0	-425.0	-205.0	-630.0					
20.0	20.0	40.0	585.0	715.0	1300.0	605.0	735.0	1340.0					
36.7	24.8	61.0	607.5	715.4	1322.0	643.0	739.0	1382.0					
-50.0	-35.0	-90.0	-150.0	20.0	-170.0	-200.0	-15.0	-215.0	.96	---------	30.6	22a	5
-225.0	-180.0	-405.0	-235.0	-75.0	-310.0	-460.0	-255.0	-715.0					
100.0	80.0	180.0	680.0	895.0	1575.0	780.0	975.0	1755.0					
100.0	80.0	180.0	680.0	895.0	1575.0	780.0	975.0	1755.0					
-31.8	-21.0	-52.0	-264.9	-285.4	-550.0	-295.0	-306.0	-601.0			30.6	22c	1

NATIONAL ADVISORY
COMMITTEE FOR AERONAUTICS

TABLE II.- MANEUVERING-FLIGHT MEASUREMENTS - Continued

Flight	Run	Time (sec)	Altitude (ft)	q_c	V_e (mph)	$n_{c.g.}$ (g)	n_t (g)	δ_e (deg)	F_e (lb)	$\dot{\theta}$ (radians/sec)	ζ (deg)	β (deg)	C_L
22c	2	-0.20	7000	Off	291	1.21	1.15	-0.7	-10.0	0	-1.9	-2.8	0.174
		.10			291	1.38	1.20	-3.3	-43.5	.085	-1.1		
		.80			287	4.84	5.26	.7	10.0	.195	3.3		
		.80			287	4.84	5.26	.7	10.0	.195	3.3		
22c	3	.70	8100	Off	290	1.18	1.15	-.6	-8.0	.005	-1.4	-1.5	.188
		.95			290	1.29	1.19	-3.9	-45.0	.080	-.6		
		1.60			290	4.73	5.16	1.0	28.0	.220	3.3		
		1.55			290	4.65	5.26	.2	20.0	.275	3.6		
22c	4	1.00	8000	Off	283	1.13	1.05	-.7	-3.5	.005	-1.1	5.8	.181
		1.30			284	1.13	.90	-2.3	-31.5	.085	-.9		
		2.10			282	4.04	4.36	-1.0	-6.0	.220	3.4		
		2.10			282	4.04	4.36	-1.0	-6.0	.220	3.4		
22c	5	-.20	8000	Off	289	1.08	1.12	-.4	-4.9	.005	-1.3	4.0	.174
		.10			289	1.33	1.06	-2.6	-33.5	.080	-.9		
		1.05			284	4.64	4.98	-1.0	1.0	.275	4.2		
		1.05			284	4.64	4.98	-1.0	1.0	.275	4.2		
23a	3	1.30	6000	.00197	373	1.22	1.12	-1.1	-7.0	-.010	-2.3	.3	.095
		1.50			373	1.53	1.21	-1.7	-26.9	.090	-2.1		
		2.65			395	5.70	6.01	0	18.5	.250	.8		
		2.60			396	5.70	5.91	0	11.1	.255	.9		
23a	4	3.20	6000	Off	382	1.18	1.00	0	-4.8	.002	-1.8	-.6	.108
		3.50			379	1.77	1.38	-1.2	-26.0	.097	-1.4		
		4.60			376	5.90	6.08	0	8.8	-------------	1.7		
		4.60			376	5.90	6.08	0	8.8	-------------	1.7		
24a	1	3.25	5000	.00202	384	1.08	1.11	----	-2.0	0	-1.3	1.8	.099
		3.60			384	1.56	1.38	----	-8.0	.050	-1.1		
		5.15			384	5.78	5.71	----	-13.7	.195	2.3		
		5.10			384	5.58	5.85	----	-4.5	.220	2.3		
24b	1	2.30	8400	.00436	264	1.11	1.00	-.4	-8.5	0	-2.2	1.5	.221
		2.60			263	1.35	.90	-4.8	-49.0	.100	-1.5		
		3.30			260	5.75	4.51	0	-10.0	.355	4.3		
		3.30			260	5.75	4.51	0	-10.0	.355	4.3		
24b	2	2.70	8000	.00354	289	1.15	1.15	-.6	-3.5	0	-2.2	1.2	.185
		3.10			289	1.37	1.15	-2.0	-30.7	.040	-1.8		
		4.00			283	6.09	6.24	0	12.9	.340	4.3		
		4.00			283	6.09	6.24	0	12.9	.340	4.3		

NATIONAL ADVISORY
COMMITTEE FOR AERONAUTICS

TABLE II.- MANEUVERING-FLIGHT MEASUREMENTS - Concluded

Tail loads (lb)									$\ddot{\theta}_{max}$ (radians/sec[2])	$\dot{\delta}_e$ (deg/sec)	c.g. (percent M.A.C.)	Flight	Run
Elevator			Stabilizer			Total							
Left	Right	Total	Left	Right	Total	Left	Right	Total					
-85.5	-43.2	-128.7	-117.6	-456.4	-574.0	-202.0	-499.0	-701.0	0.64	---------	30.6	22c	2
-249.3	-186.7	-435.9	-109.0	-393.8	-502.8	-358.0	-579.0	-937.0					
124.6	138.7	263.3	857.8	364.7	1222.5	981.0	502.0	1483.0					
124.6	138.7	263.3	857.8	364.7	1222.5	981.0	502.0	1483.0					
-84.7	-30.2	-114.9	-157.5	-393.8	-551.4	-241.0	-424.0	-655.0	.64	---------	30.6	22c	3
-255.0	-160.0	-410.0	-190.0	-420.0	-610.0	-445.0	-580.0	-1025.0					
137.6	165.6	303.2	821.1	392.8	1213.9	958.0	557.0	1515.0					
140.0	160.0	300.0	870.0	410.0	1285.0	1010.0	570.0	1580.0					
-81.7	-43.0	-125.0	-369.0	-125.3	-494.2	-450.0	-168.0	-620.0	.48	---------	30.6	22c	4
-201.5	-161.9	-363.4	-412.2	-164.0	-576.2	-613.0	-325.0	-938.0					
12.1	46.7	58.8	297.8	595.6	893.4	309.0	632.0	942.0					
12.1	46.7	58.8	297.8	595.6	893.4	309.0	632.0	942.0					
-91.2	-29.4	-120.6	-355.0	-178.0	-533.0	-446.0	-207.0	-653.0	.48	---------	30.6	22c	5
-186.1	-168.3	-354.5	-351.8	-168.3	-520.1	-573.0	-336.0	-909.0					
55.0	80.0	135.0	435.0	720.0	1145.0	490.0	800.0	1290.0					
55.0	80.0	135.0	435.0	720.0	1145.0	490.0	800.0	1290.0					
-130.0	-55.0	-185.0	-444.0	-894.0	-1338.0	-574.0	-949.0	-1523.0	.48	---------	30.6	23a	3
-230.0	-149.0	-379.0	-373.0	-824.0	-1202.0	-603.0	-973.0	-1576.0					
120.0	190.0	310.0	770.0	80.0	850.0	890.0	270.0	1160.0					
53.0	110.0	163.0	768.0	113.0	881.0	821.0	223.0	1044.0					
-60.0	-20.0	-80.0	-405.0	-655.0	-1060.0	-465.0	-675.0	-1140.0	.28	---------	30.6	23a	4
-168.3	-110.1	-278.4	-407.9	-598.9	-1006.7	-575.0	-708.0	-1284.0					
140.3	179.7	319.9	657.1	384.1	1041.2	797.0	563.0	1360.0					
140.3	179.7	319.9	657.1	384.1	1041.2	797.0	563.0	1360.0					
-55.0	15.0	-40.0	-455.0	-545.0	-1025.0	-510.0	-530.0	-1040.0	.28	---------	30.6	24a	1
-53.4	-11.3	-64.7	-487.7	-576.2	-1063.9	-540.0	-587.0	-1127.0					
70.0	140.0	210.0	470.0	360.0	830.0	540.0	500.0	1040.0					
61.5	121.4	182.9	485.6	384.1	869.7	546.0	505.0	1051.0					
-55.0	-40.0	-95.0	-140.0	-320.0	-480.0	-150.0	-360.0	-510.0	1.08	---------	30.6	24b	1
-271.9	-241.2	-513.1	-180.2	-355.0	-535.2	-451.0	-596.0	-1047.0					
139.2	146.7	285.9	974.3	637.7	1612.0	1113.0	783.0	1896.0					
139.2	146.7	285.9	974.3	637.7	1612.0	1113.0	783.0	1896.0					
-56.7	-5.4	-62.0	-194.2	-371.2	-565.4	-250.0	-376.0	-626.0	.64	---------	30.6	24b	2
-193.1	-129.5	-322.6	-199.6	-424.1	-623.7	-392.0	-553.0	-945.0					
182.4	197.5	379.8	1076.3	696.0	1772.3	1258.0	893.0	2151.0					
182.4	197.5	379.8	1076.3	696.0	1772.3	1258.0	893.0	2151.0					

NATIONAL ADVISORY
COMMITTEE FOR AERONAUTICS

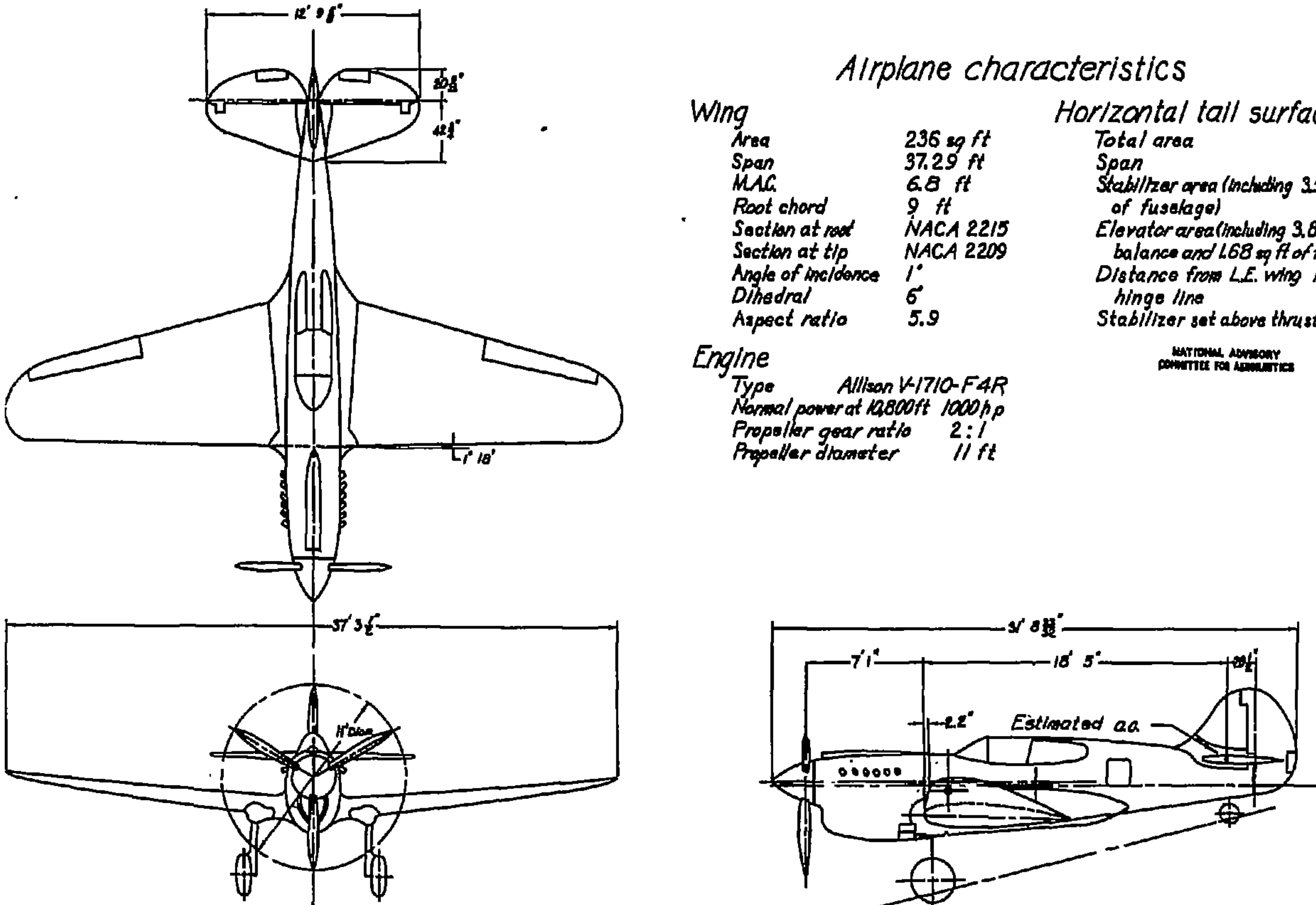

Figure 1.- Three-view drawing and details of the airplane used in tail-loads investigation.

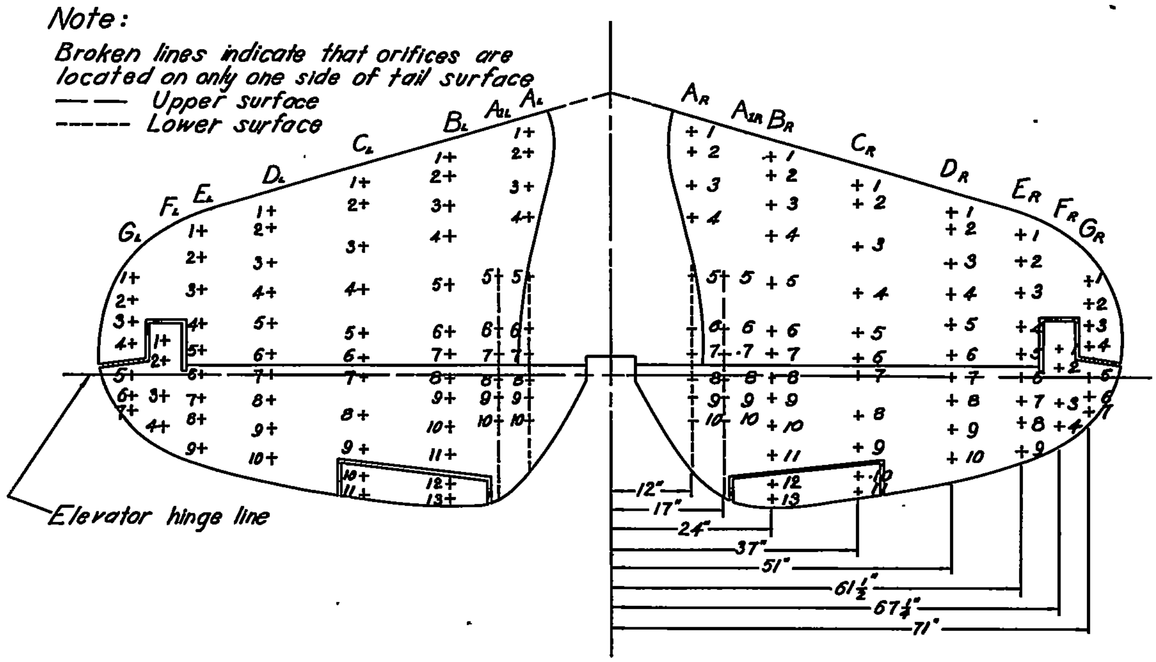

NATIONAL ADVISORY
COMMITTEE FOR AERONAUTICS

Rib	Chord	Orifice location in percent of chord from leading edge												
		1	2	3	4	5	6	7	8	9	10	11	12	13
A_R	53.5	4.2	9.8	21.0	29.0	45.8	61.1	67.8	75.3	80.4	87.0			
A_{1R}	57.25					40.1	54.6	61.1	67.6	72.9	79.0			
B_R	56.5	4.4	9.7	17.7	25.7	38.9	51.7	57.9	64.6	69.9	77.5	85.8	92.9	97.4
C_R	51.0	5.9	11.8	24.5	38.2	50.5	58.3	63.7	75.5	84.9	93.2	98.0		
D_R	44.5	6.8	12.4	24.7	35.4	45.6	56.2	63.5	71.9	81.5	92.2			
E_R	38.5	9.1	19.5	32.5	45.5	56.5	65.6	74.6	83.1	94.8				
F_R	33.5	53.8	62.7	79.1	89.6									
G_R	26.0	15.4	28.8	42.3	53.8	71.1	83.7	92.2						
A_L	53.5	3.7	9.8	20.6	28.5	45.3	60.7	67.8	74.8	80.4	89.7			
A_{1L}	57.25					39.7	54.6	60.7	67.2	73.8	83.0			
B_L	56.5	4.0	9.3	16.8	25.7	39.4	50.4	57.0	64.6	70.8	77.9	86.3	92.9	98.2
C_L	51.0	5.4	11.8	24.5	38.2	50.5	58.3	64.2	75.5	85.3	93.6	99.0		
D_L	44.5	6.7	12.4	24.7	35.4	45.5	56.2	64.0	71.9	82.0	92.1			
E_L	38.5	9.1	19.5	32.5	45.5	57.1	64.9	74.6	83.8	95.4				
F_L	33.5	53.0	62.7	79.1	89.6									
G_L	26.0	13.5	28.8	43.3	54.8	72.1	83.7	93.2						

Figure 2.- Orifice locations on horizontal tail of test airplane.

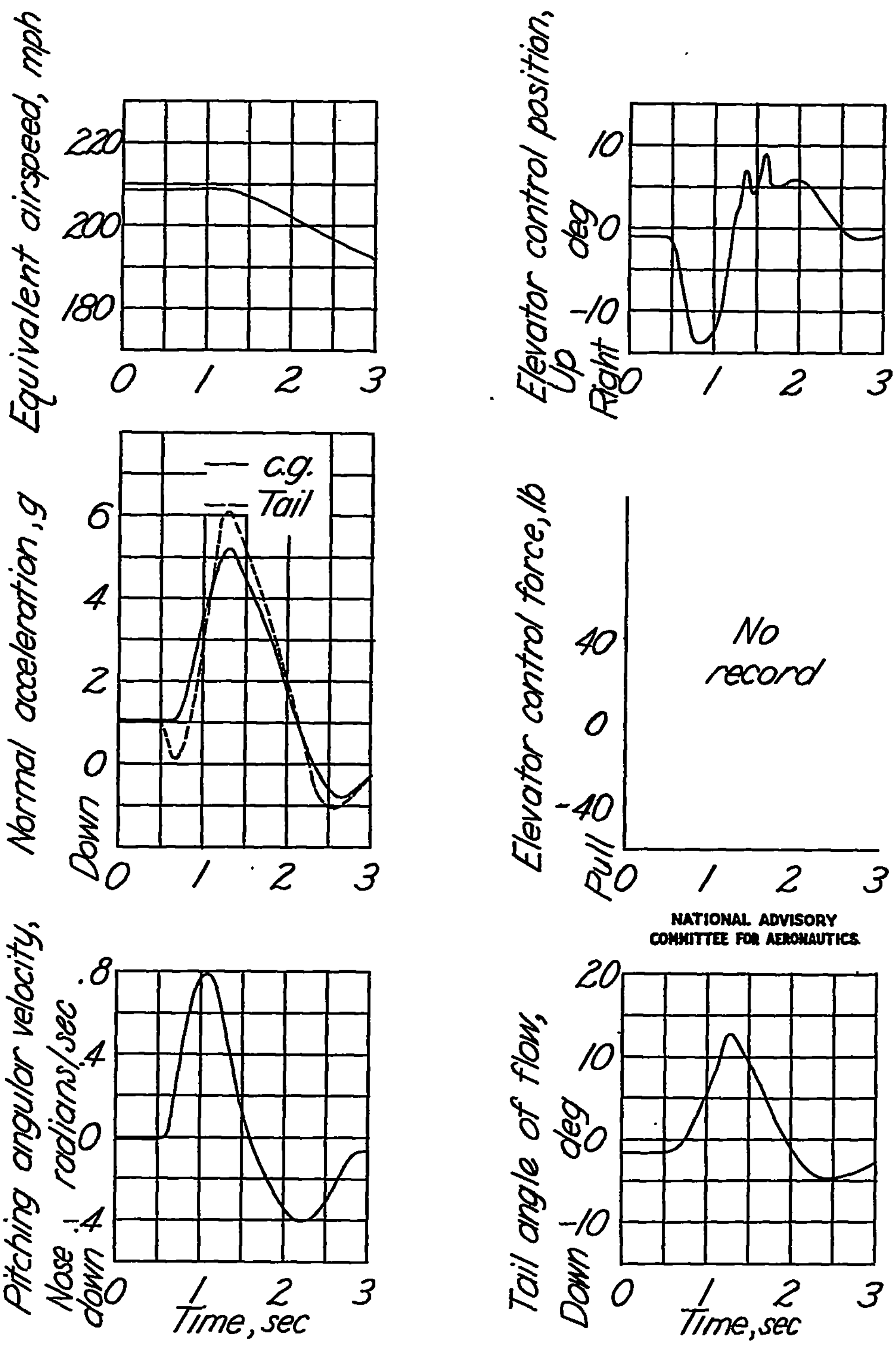

Figure 3.- Time variation of pertinent quantities measured during a stalled pull-up of the test airplane with center of gravity at 29.7 percent mean aerodynamic chord; power on; engine speed, 2620 rpm; altitude, 6970 feet; manifold pressure, 24.0 inches Hg; flight 16a, run 3.

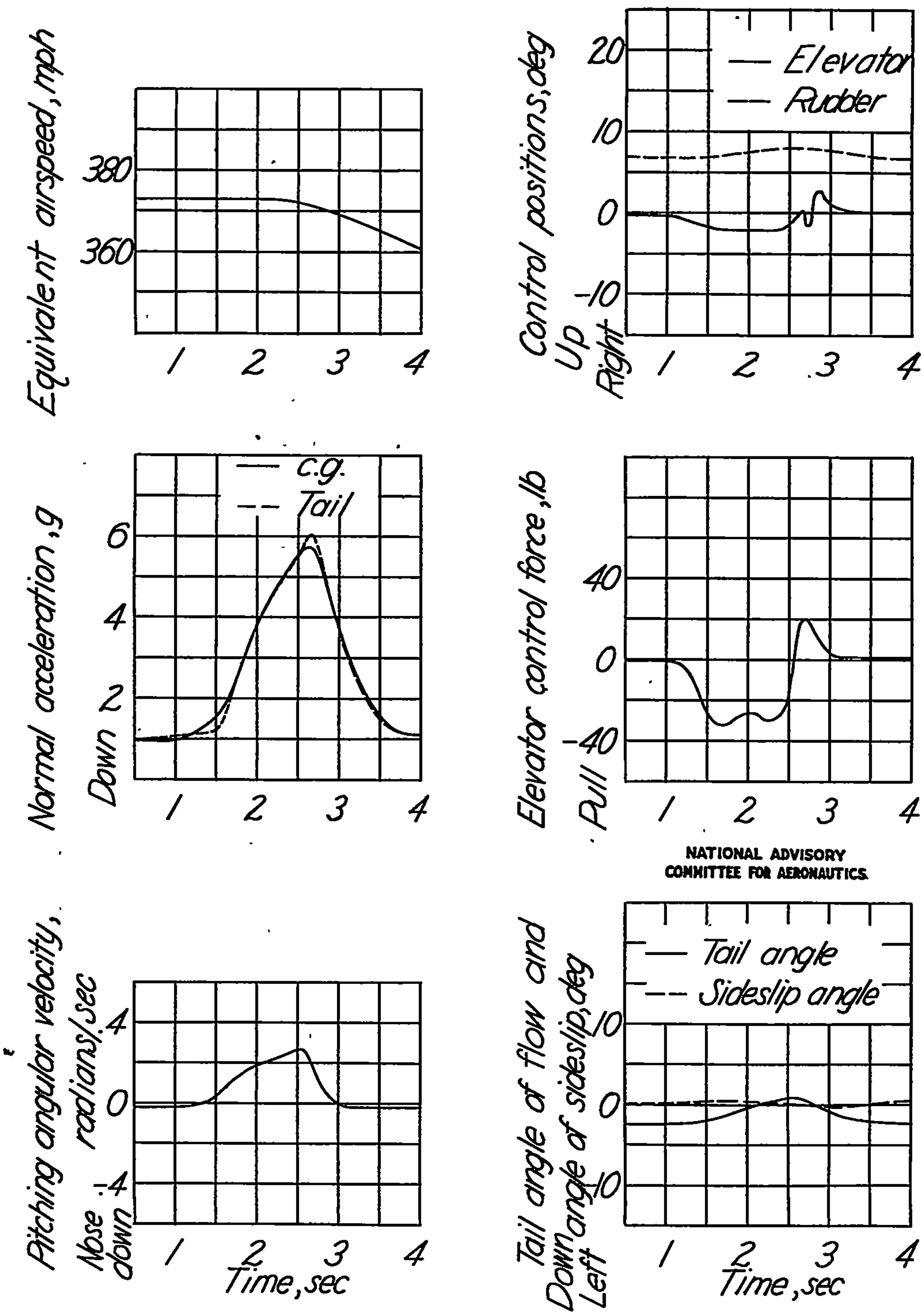

Figure 4.- Time variation of pertinent quantities measured during a typical pull-up of the test airplane with center of gravity at 30.6 percent mean aerodynamic chord; power on; engine speed, 2600 rpm; altitude, 6000 feet; manifold pressure, 36.0 inches Hg; flight 23a, run 3.

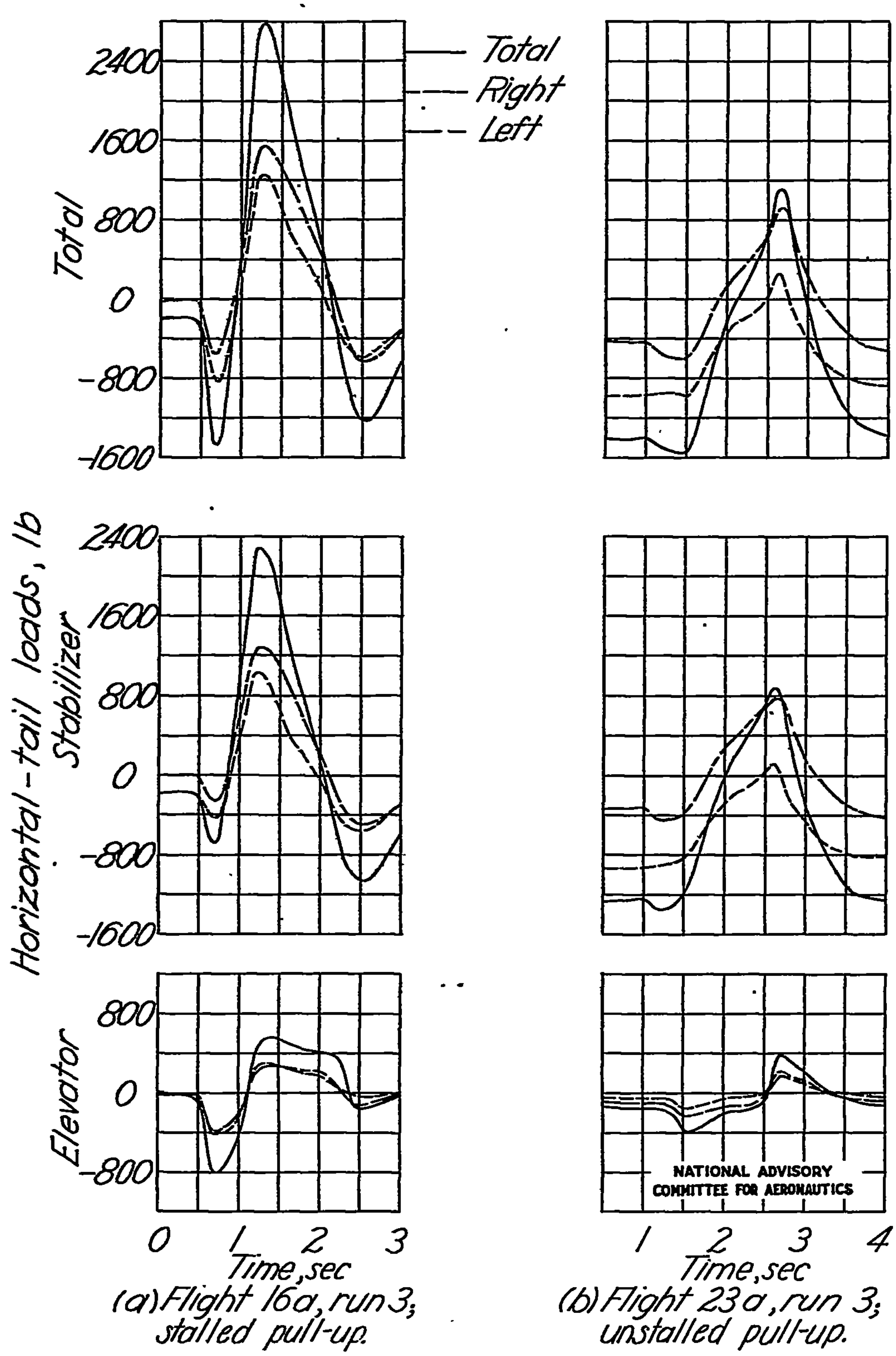

Figure 5.- Time variation of aerodynamic loads on horizontal tail surface.

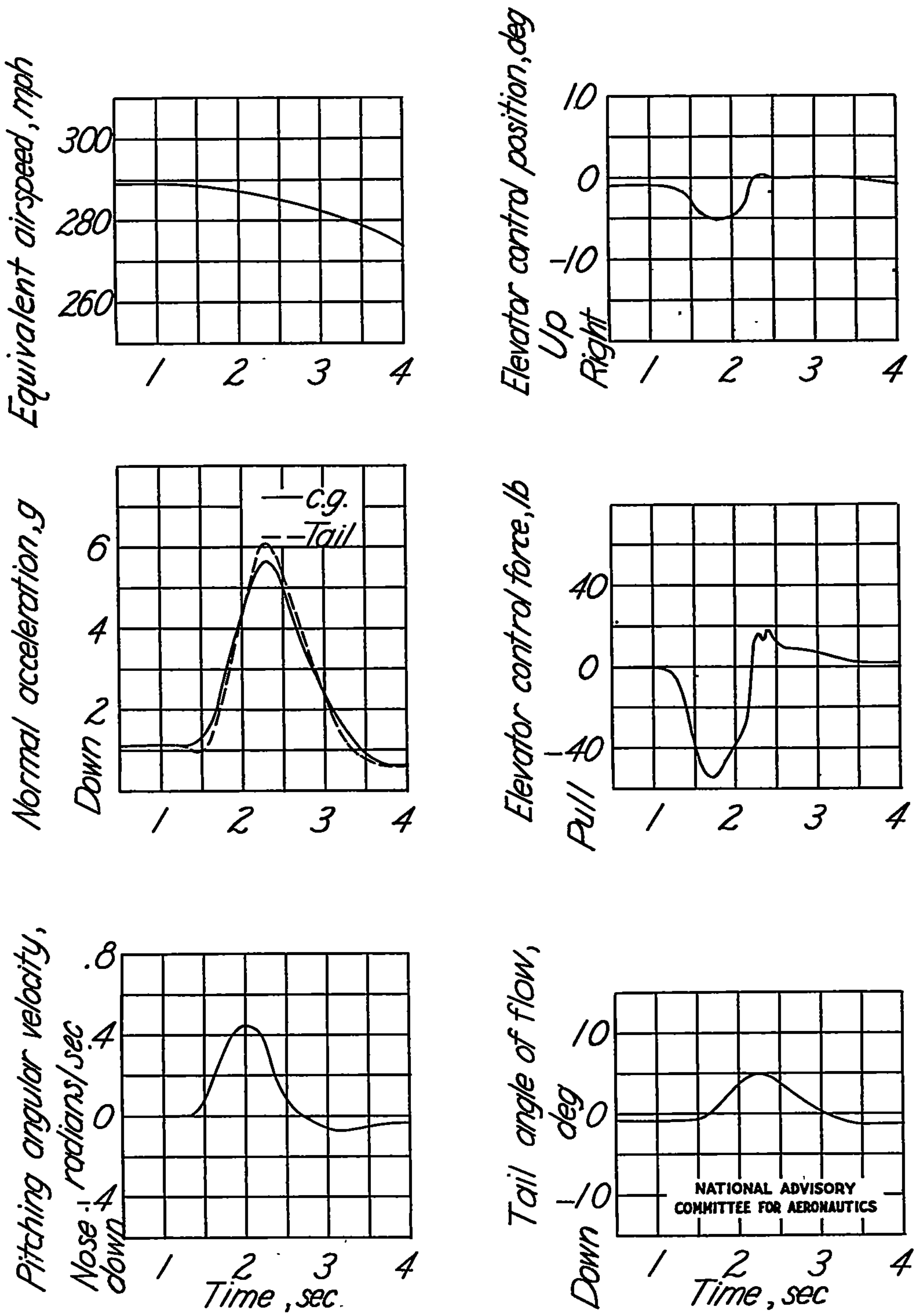

Figure 6.- Time variation of pertinent quantities measured during a typical pull-up of the test airplane with center of gravity at 29.7 percent mean aerodynamic chord; power on; engine speed, 2600 rpm; altitude, 7000 feet; manifold pressure, 36.5 inches Hg; flight 20, run 2.

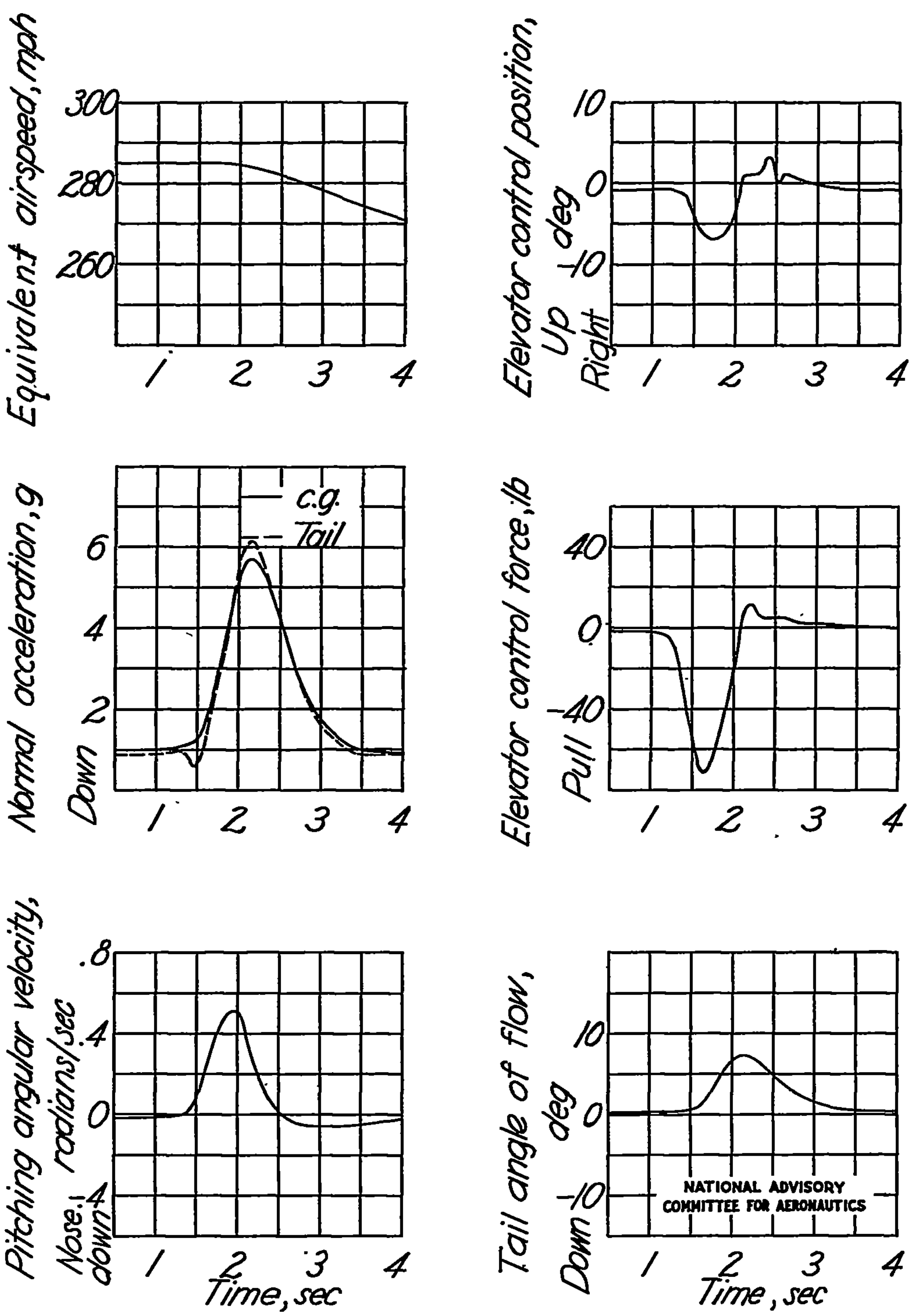

Figure 7.- Time variation of pertinent quantities measured during a typical pull-up of the test airplane with center of gravity at 29.7 percent mean aerodynamic chord; power off; engine speed, 2600 rpm; altitude, 7500 feet; flight 20, run 7.

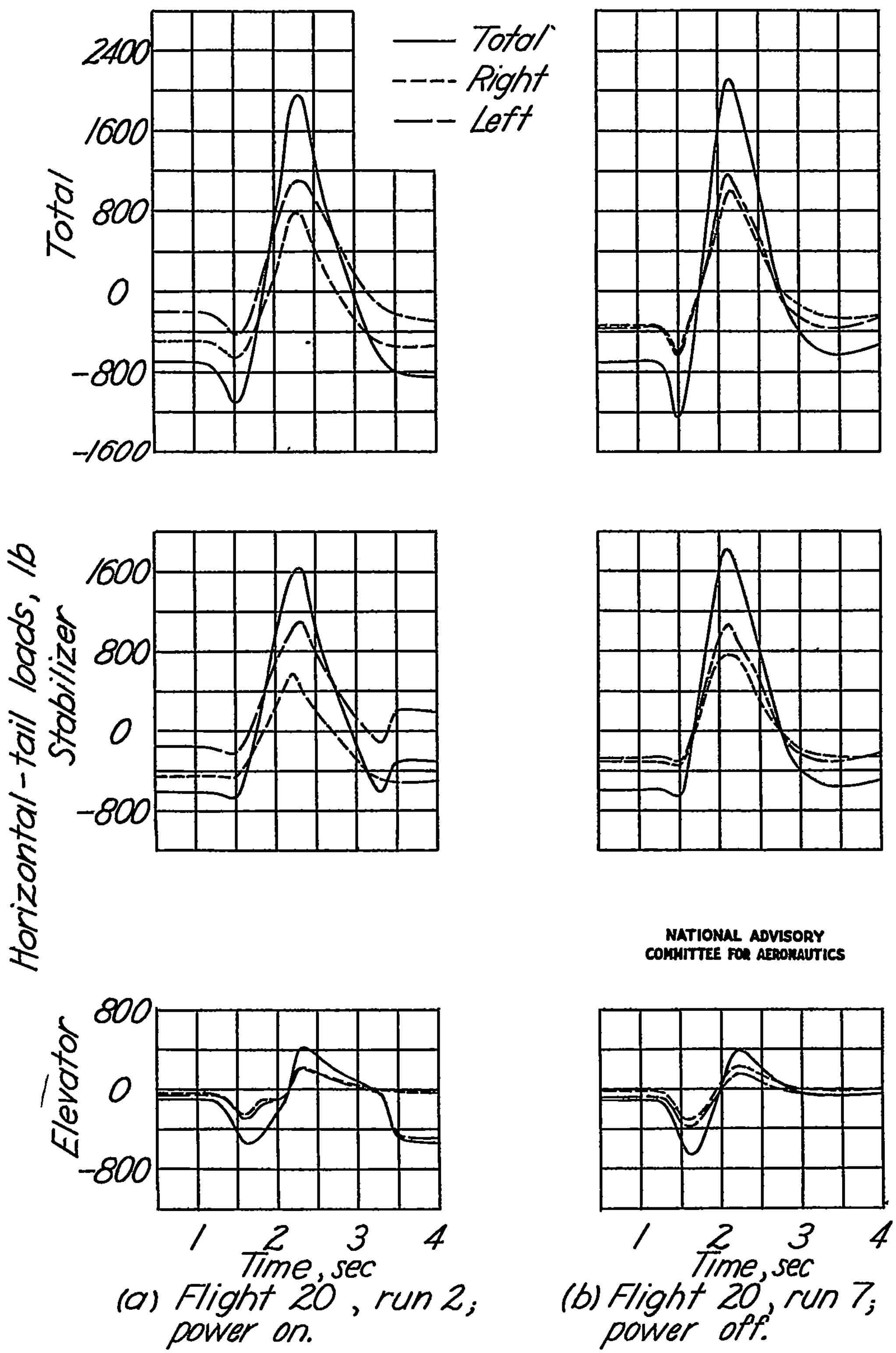

Figure 8.- Time variation of aerodynamic loads on horizontal tail surfaces.

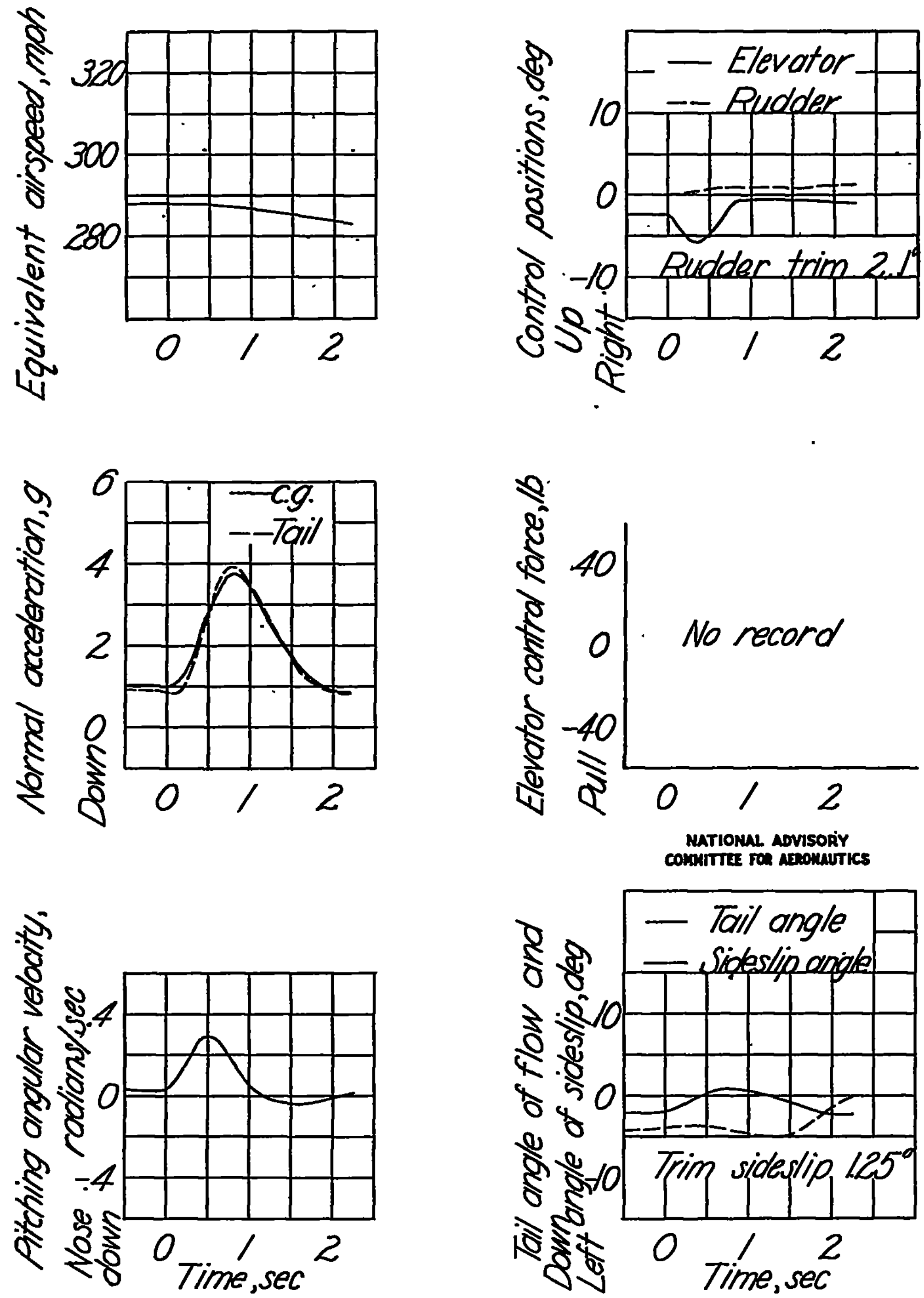

Figure 9.- Time variation of pertinent quantities measured during a typical pull-up from a steady sideslip of the test airplane with center of gravity at 30.6 percent mean aerodynamic chord; power on; engine speed, 2600 rpm; altitude, 7300 feet; manifold pressure, 37.0 inches Hg; flight 21b, run 2.

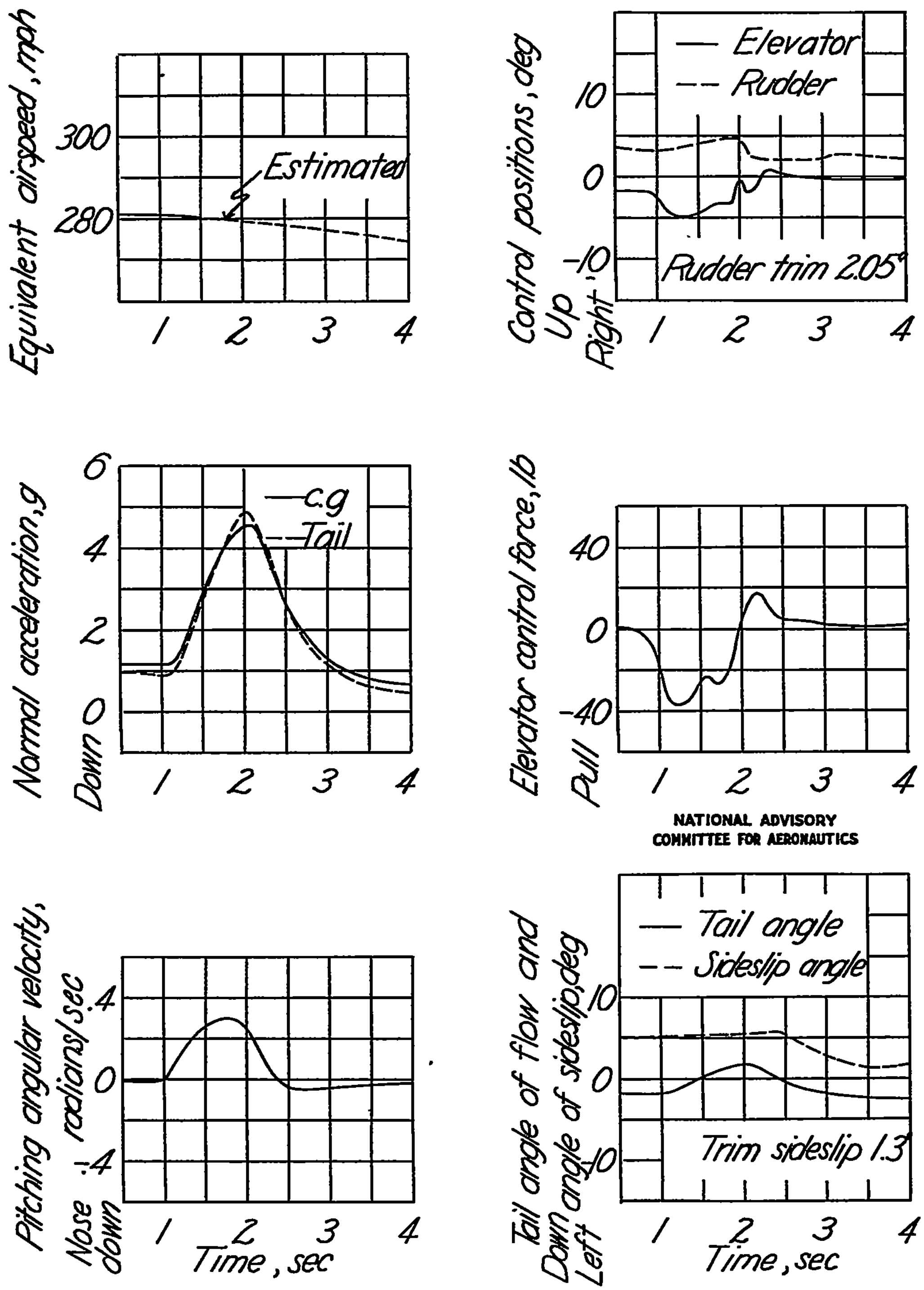

Figure 10.- Time variation of pertinent quantities measured during a typical pull-up from a steady sideslip of the test airplane with center of gravity at 30.6 percent mean aerodynamic chord; power on; engine speed, 2600 rpm; altitude, 8500 feet; manifold pressure, 36.0 inches Hg; flight 21b, run 5.

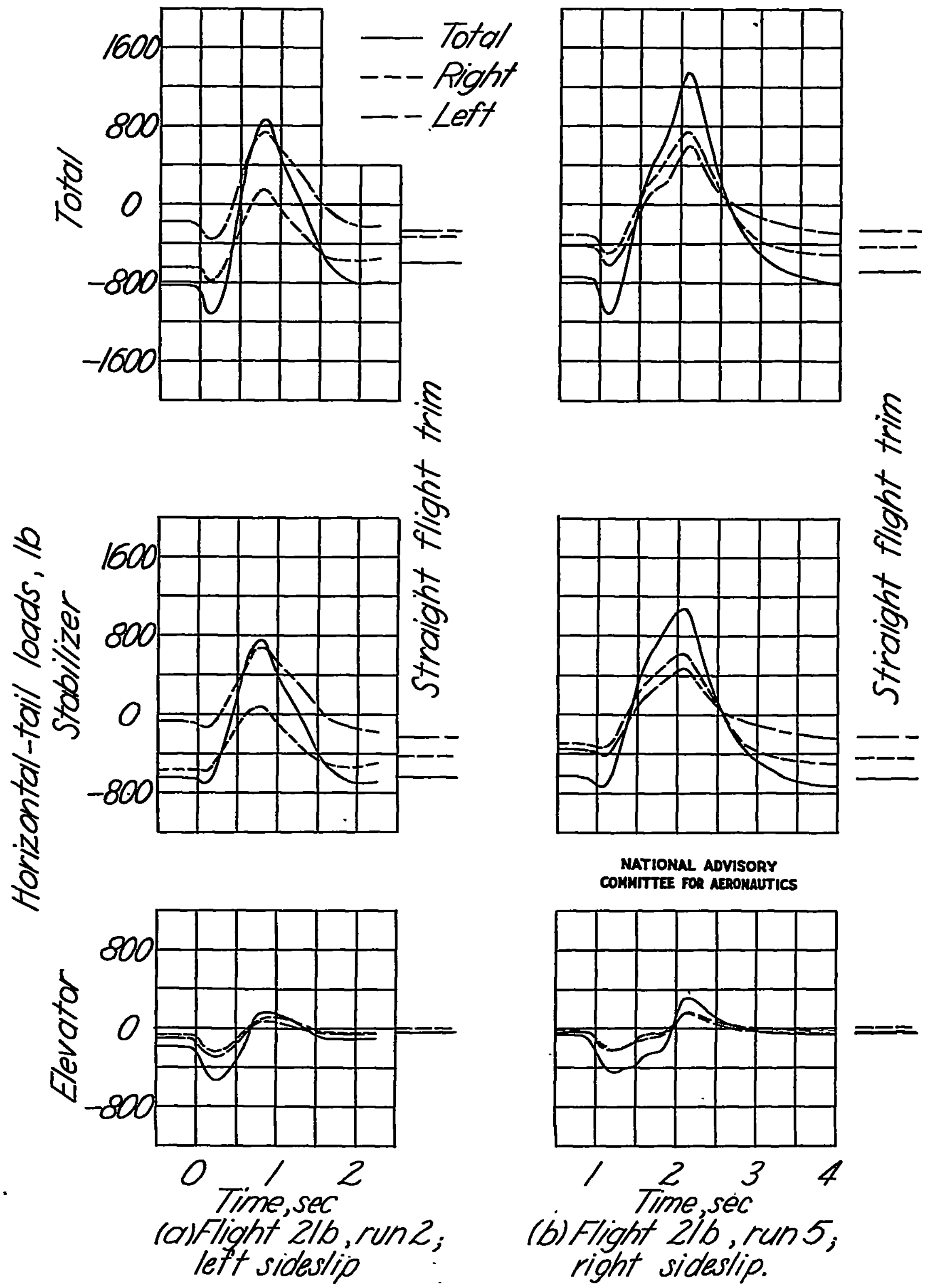

Figure 11.- Time variation of aerodynamic loads on horizontal tail surfaces, power on.

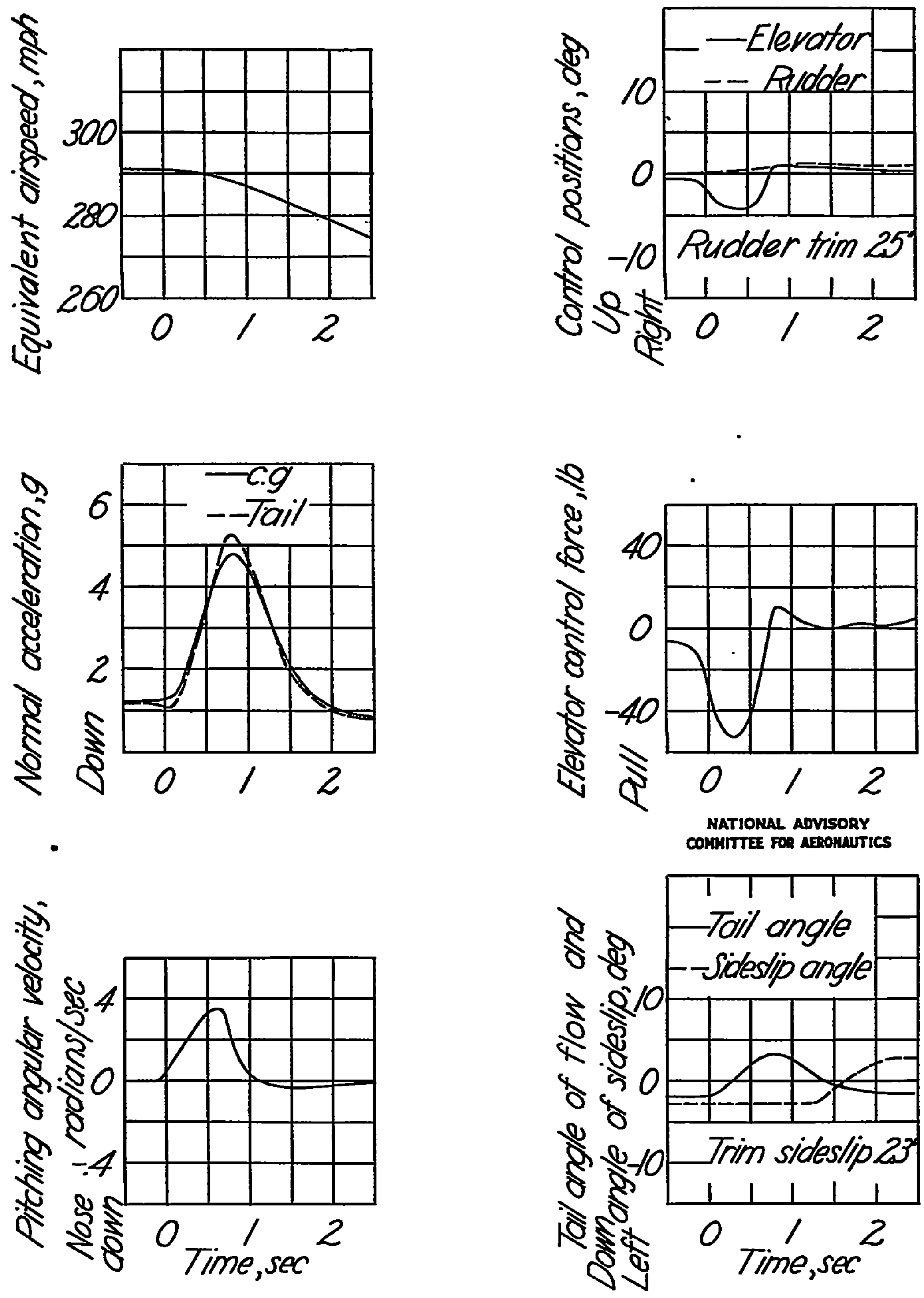

Figure 12.- Time variation of pertinent quantities measured during a typical pull-up from a steady sideslip of the test airplane with center of gravity at 30.6 percent mean aerodynamic chord; power off; engine speed, 2600 rpm; altitude, 7000 feet; flight 22c, run 2.

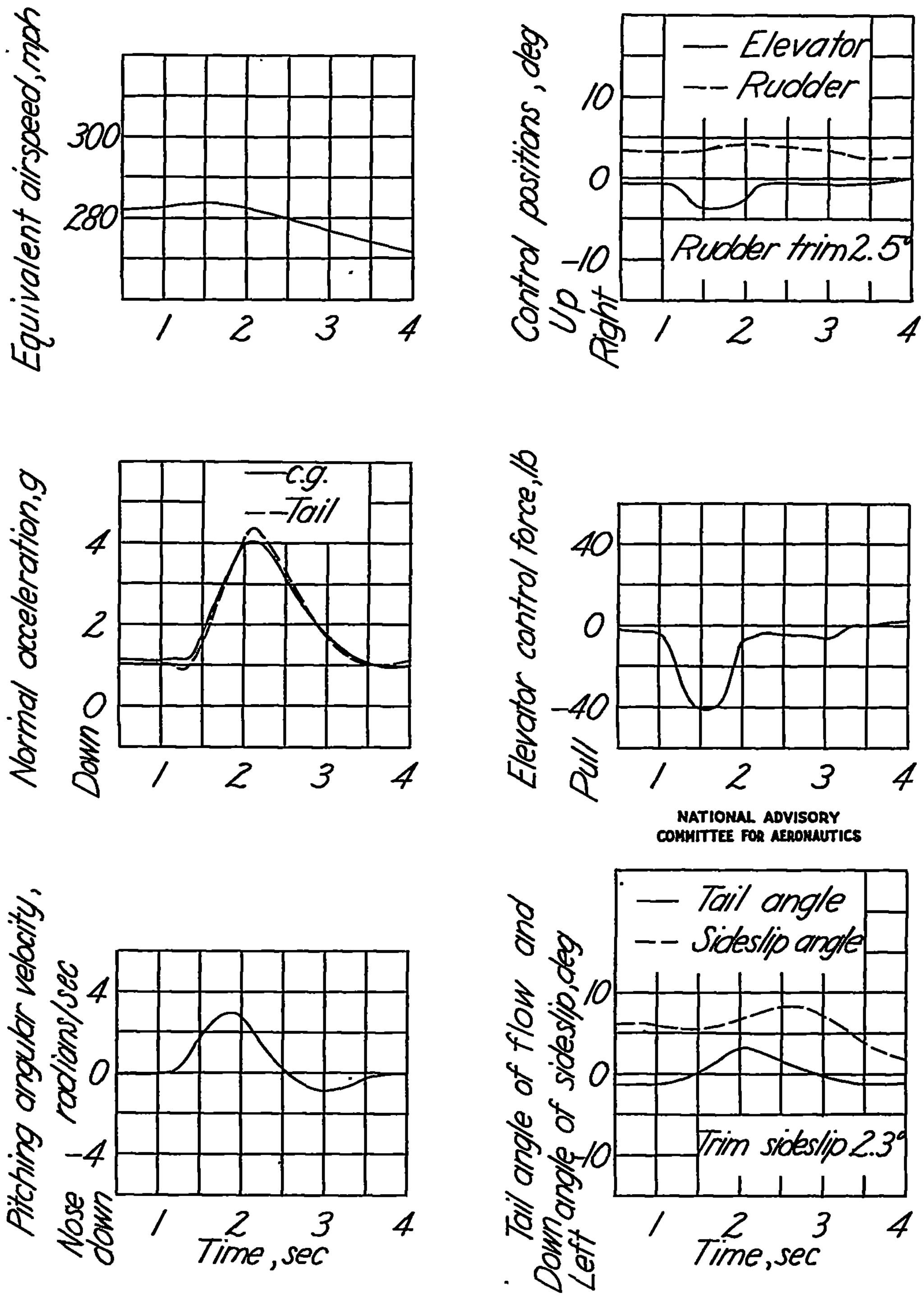

Figure 13.- Time variation of pertinent quantities measured during a typical pull-up from a steady sideslip of the test airplane with center of gravity at 30.6 percent mean aerodynamic chord; power off; engine speed, 2600 rpm; altitude, 8000 feet; flight 22c, run 4.

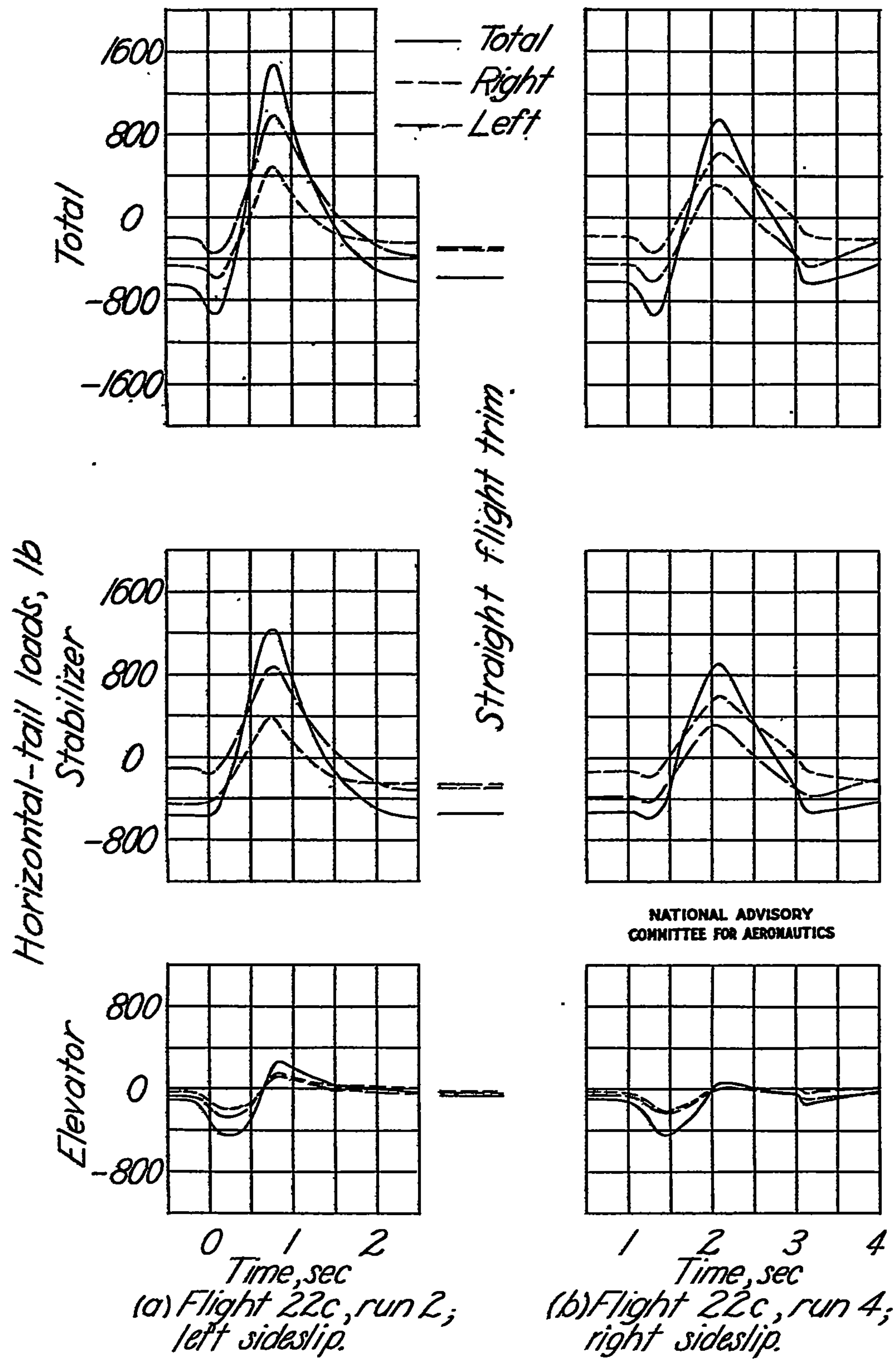

Figure 14.- Time variation of aerodynamic loads on horizontal tail surface, power off.

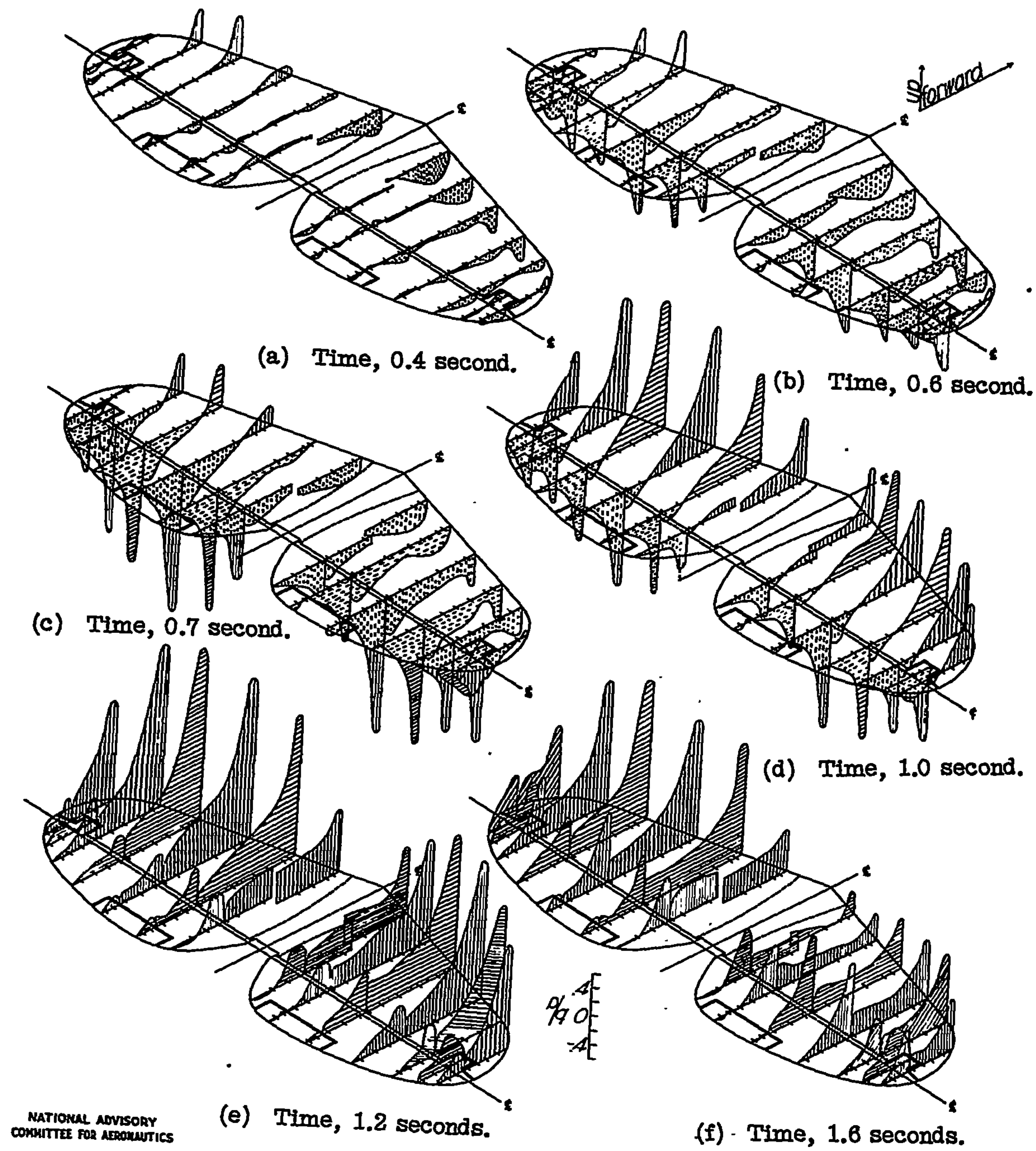

Figure 15.- Isometric views of differential pressure distribution over the horizontal tail surface of the test airplane for flight 16a, run 3.

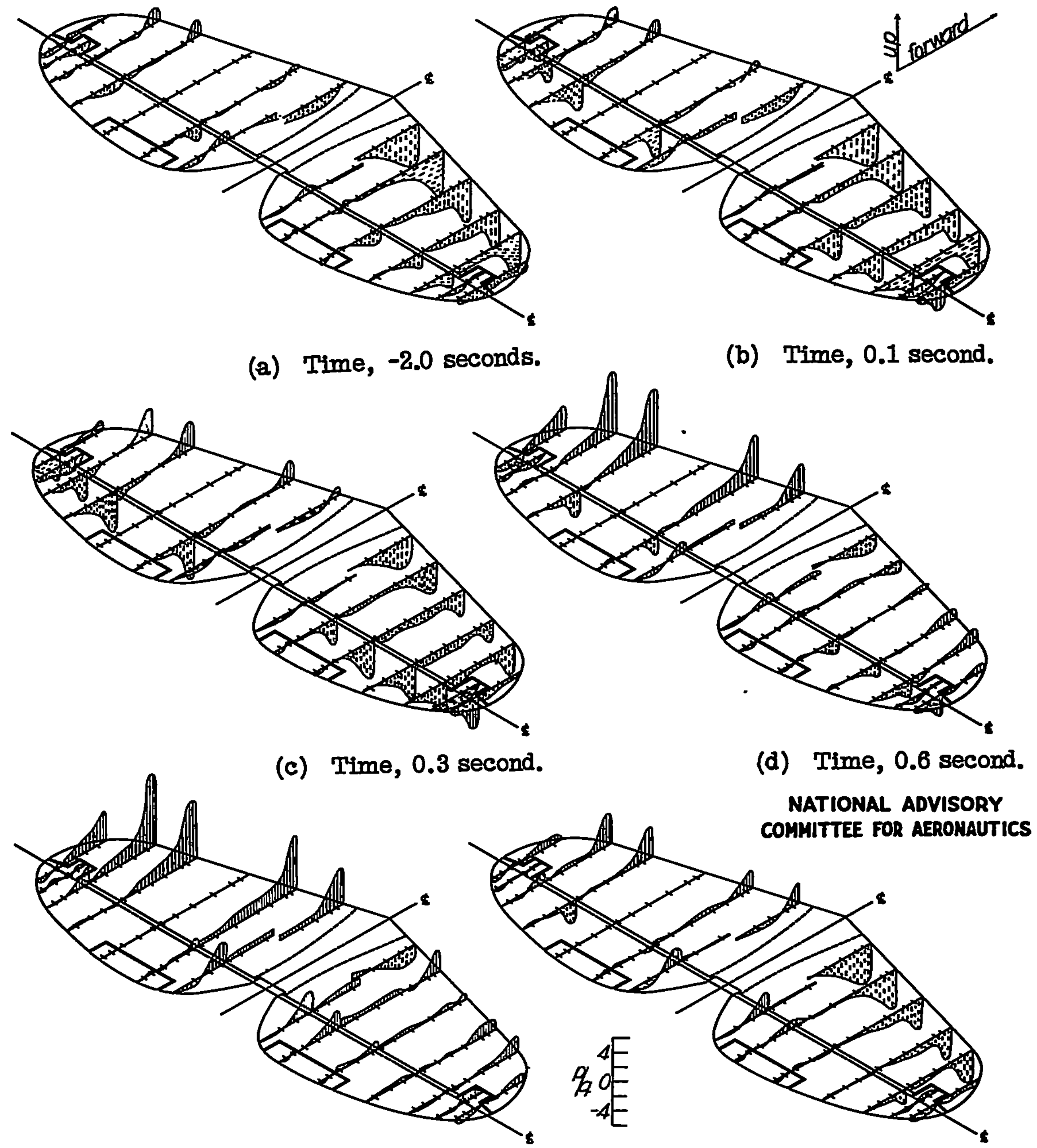

(a) Time, -2.0 seconds.

(b) Time, 0.1 second.

(c) Time, 0.3 second.

(d) Time, 0.6 second.

(e) Time, 0.8 second.

(f) Time, 1.4 seconds.

NATIONAL ADVISORY
COMMITTEE FOR AERONAUTICS

Figure 16.- Isometric views of differential pressure distribution over the horizontal tail surface of the test airplane for flight 21b, run 2.

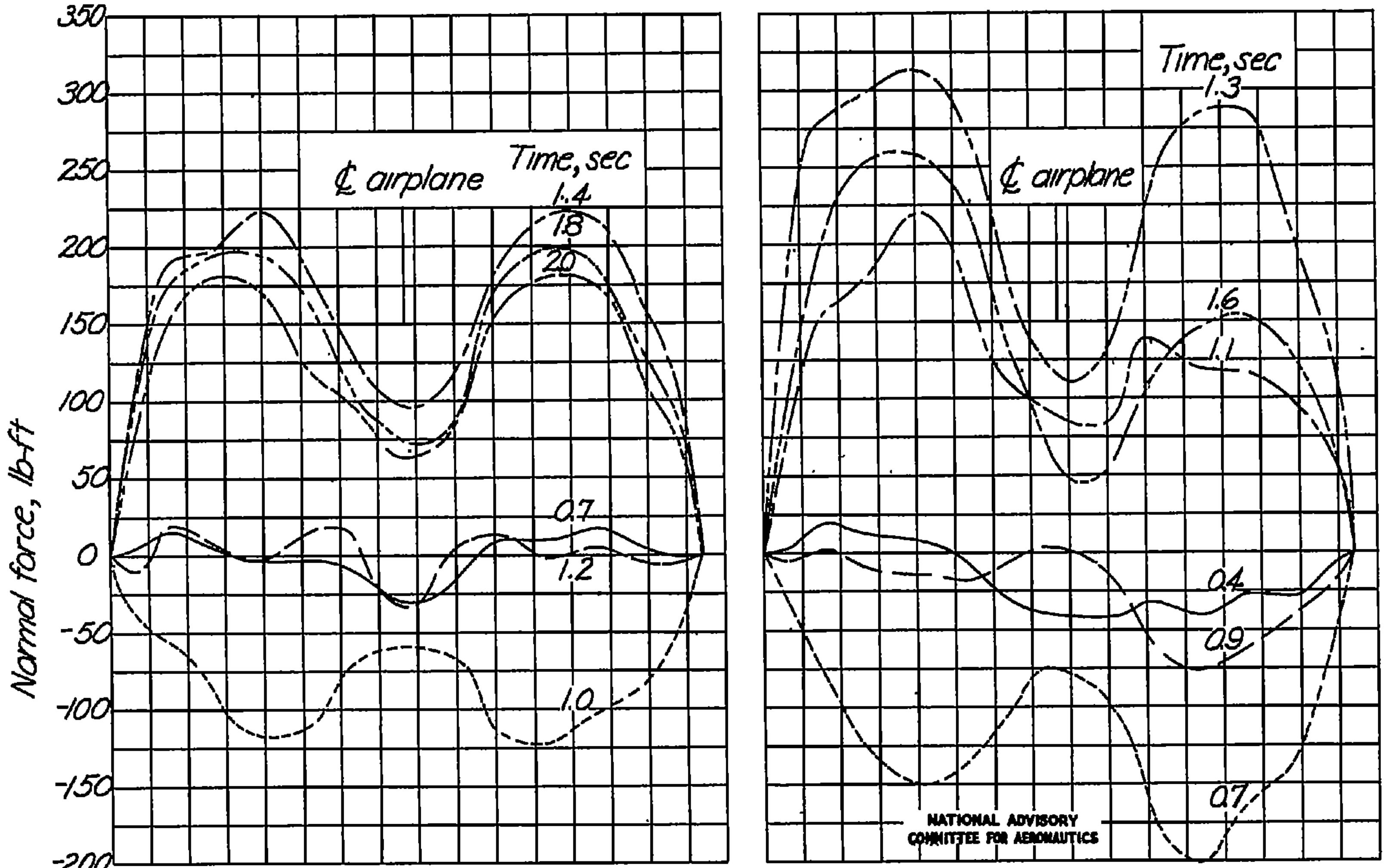

(a) Flight 15, run 6; power off.

(b) Flight 16a, run 3; power on.

Figure 17.- Spanwise normal-force distributions over the horizontal tail.

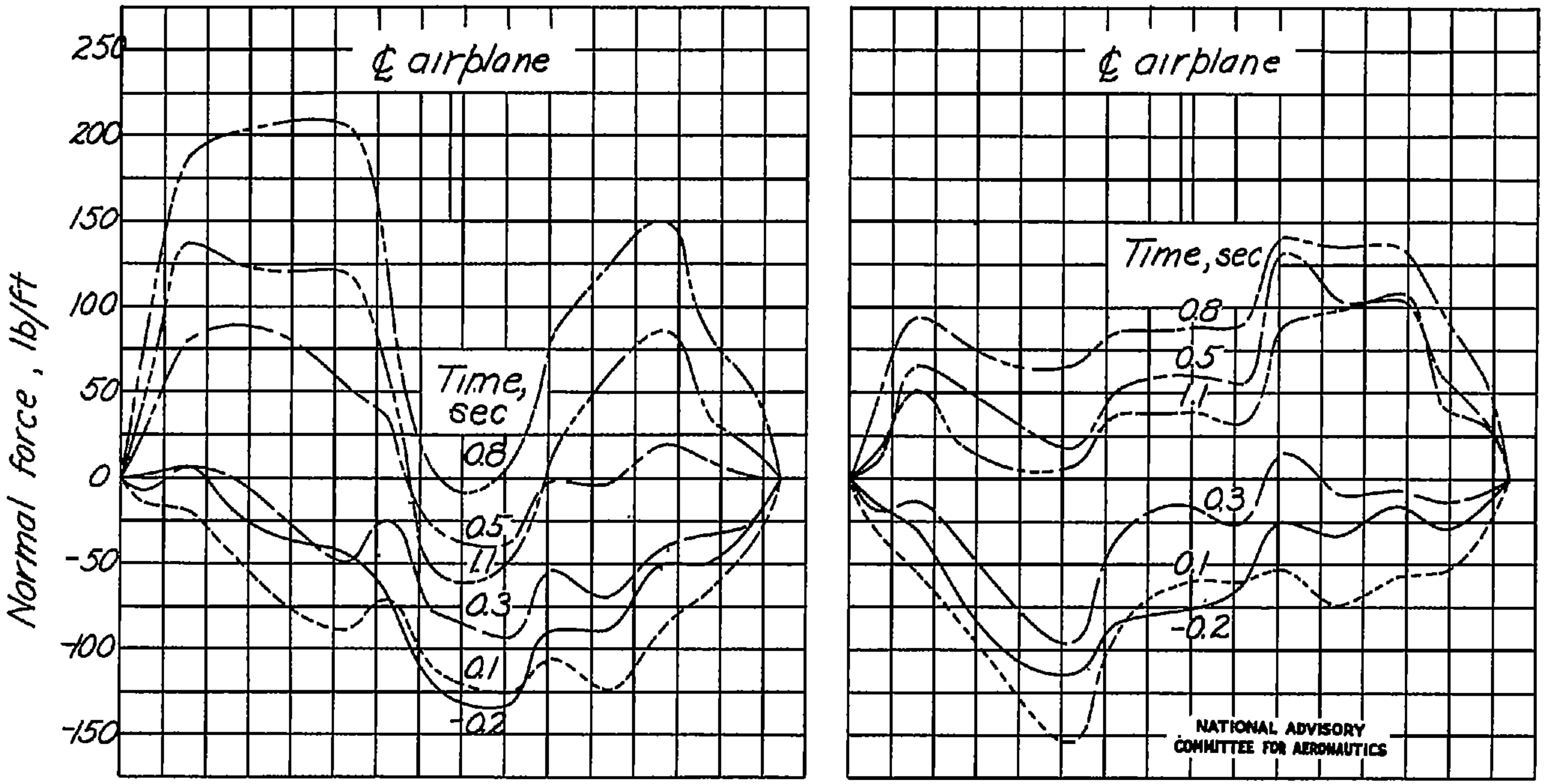

(a) Flight 22c, run 2 (-28° left sideslip). (b) Flight 22c, run 5 (40° right sideslip).

Figure 18.- Spanwise normal-force distributions over the horizontal tail.

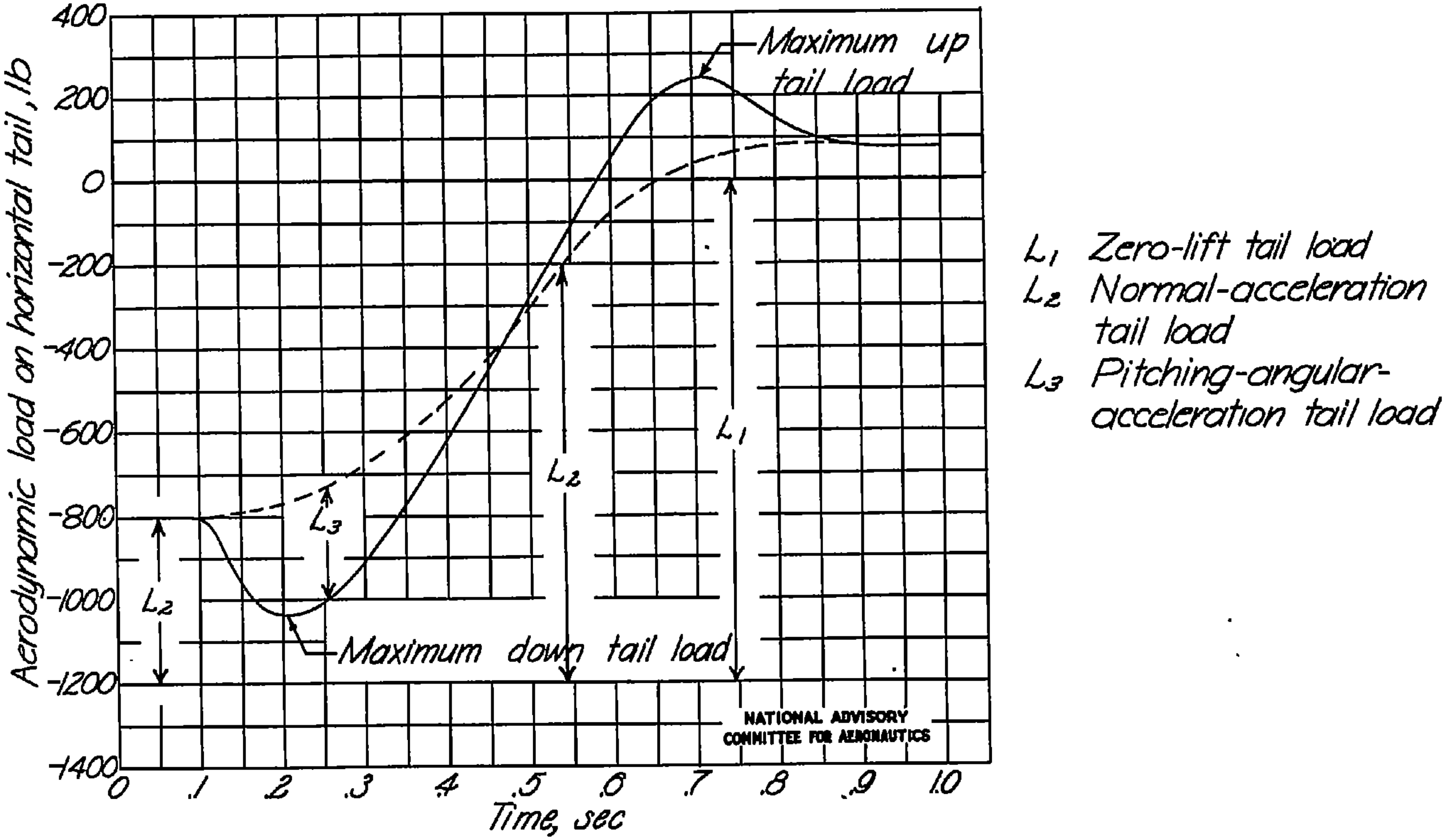

Figure 19.- Tail-load nomenclature and sequence for an arbitrary pull-up maneuver. (Assumed no loss in speed.)

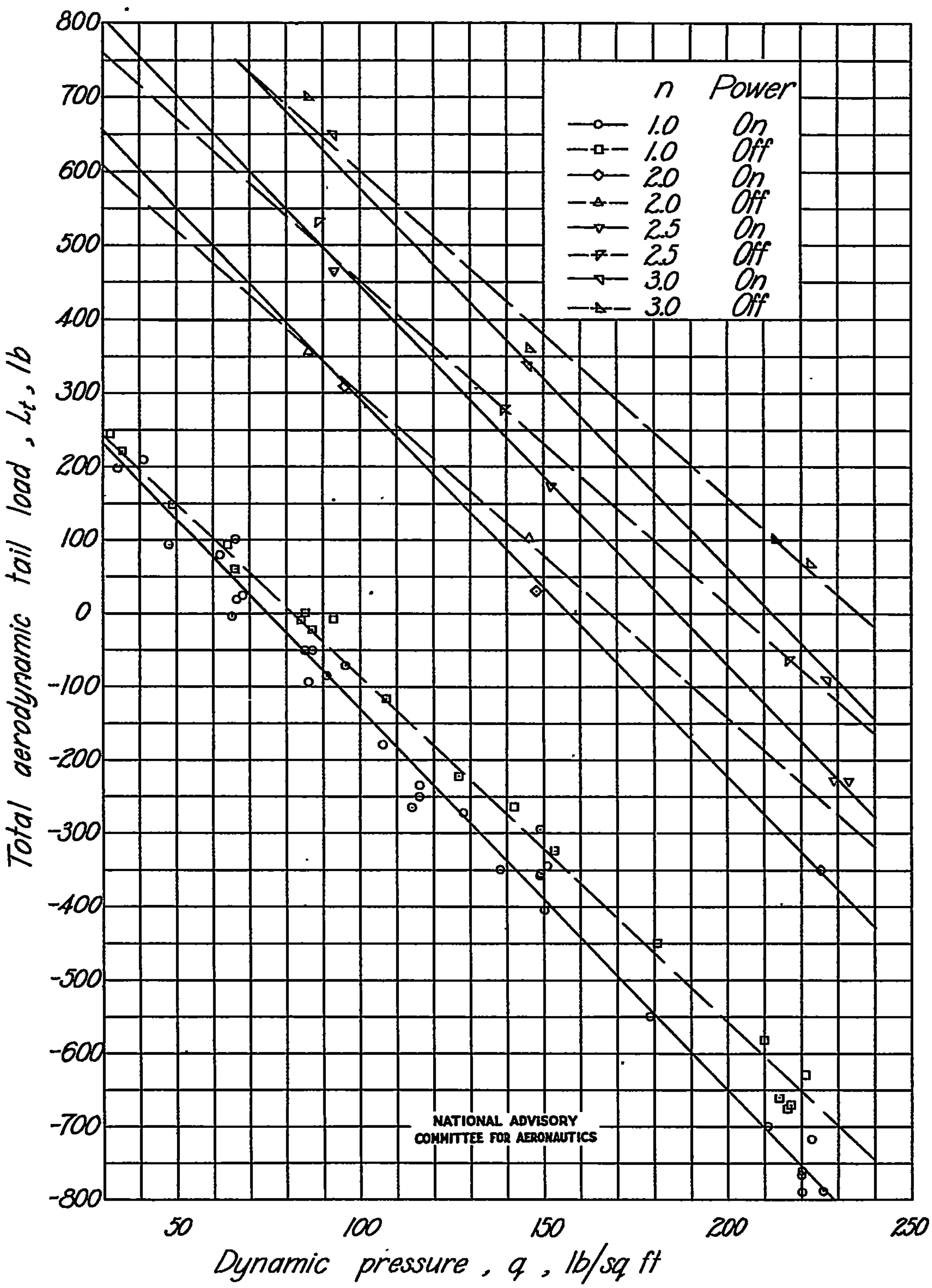

Figure 20.- Variation of aerodynamic tail load with power condition, normal acceleration, and dynamic pressure for test airplane with center of gravity at 29.7 percent mean aerodynamic chord.

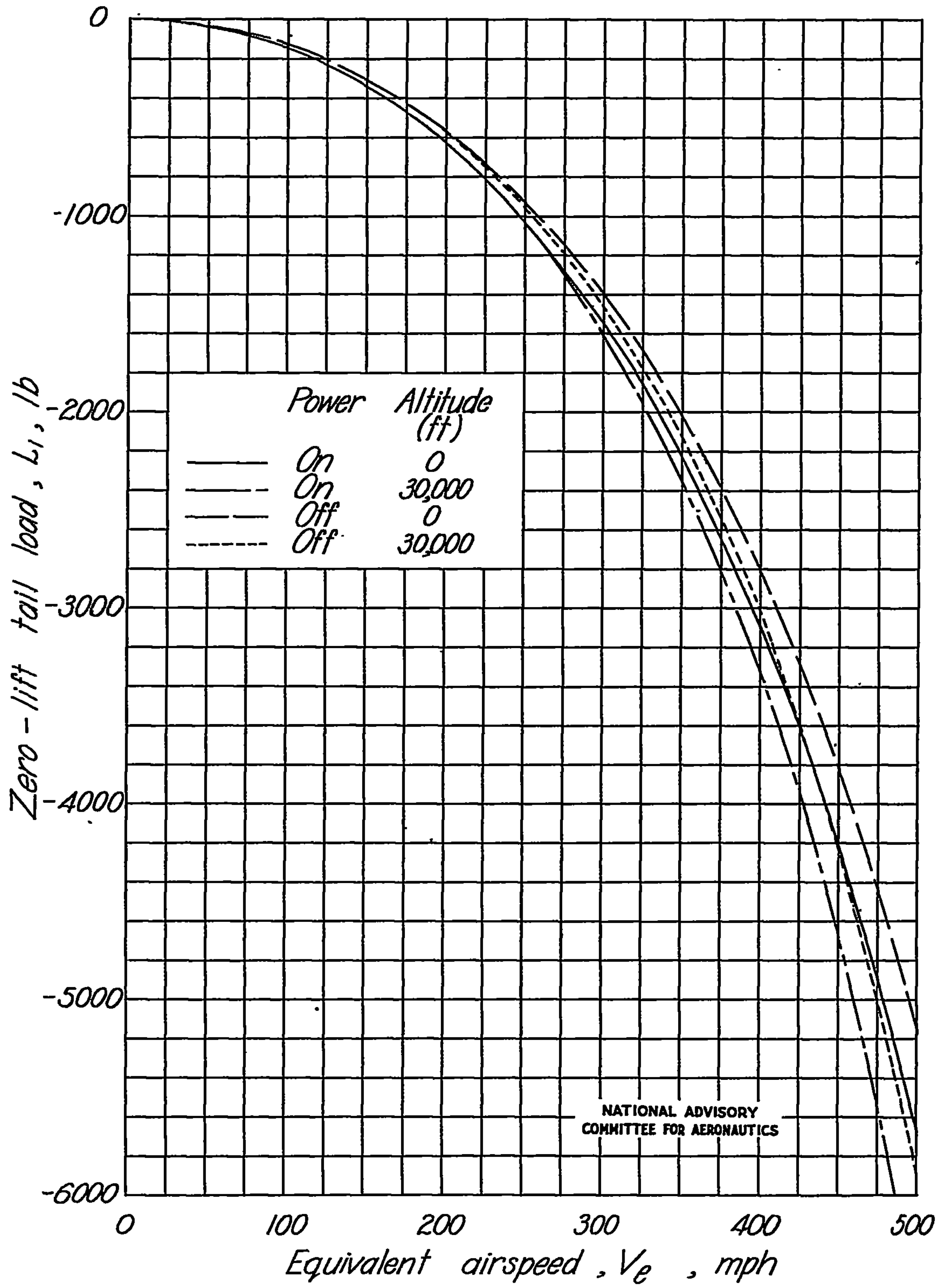

Figure 21.- Horizontal-tail load for zero-lift flight in the test airplane.

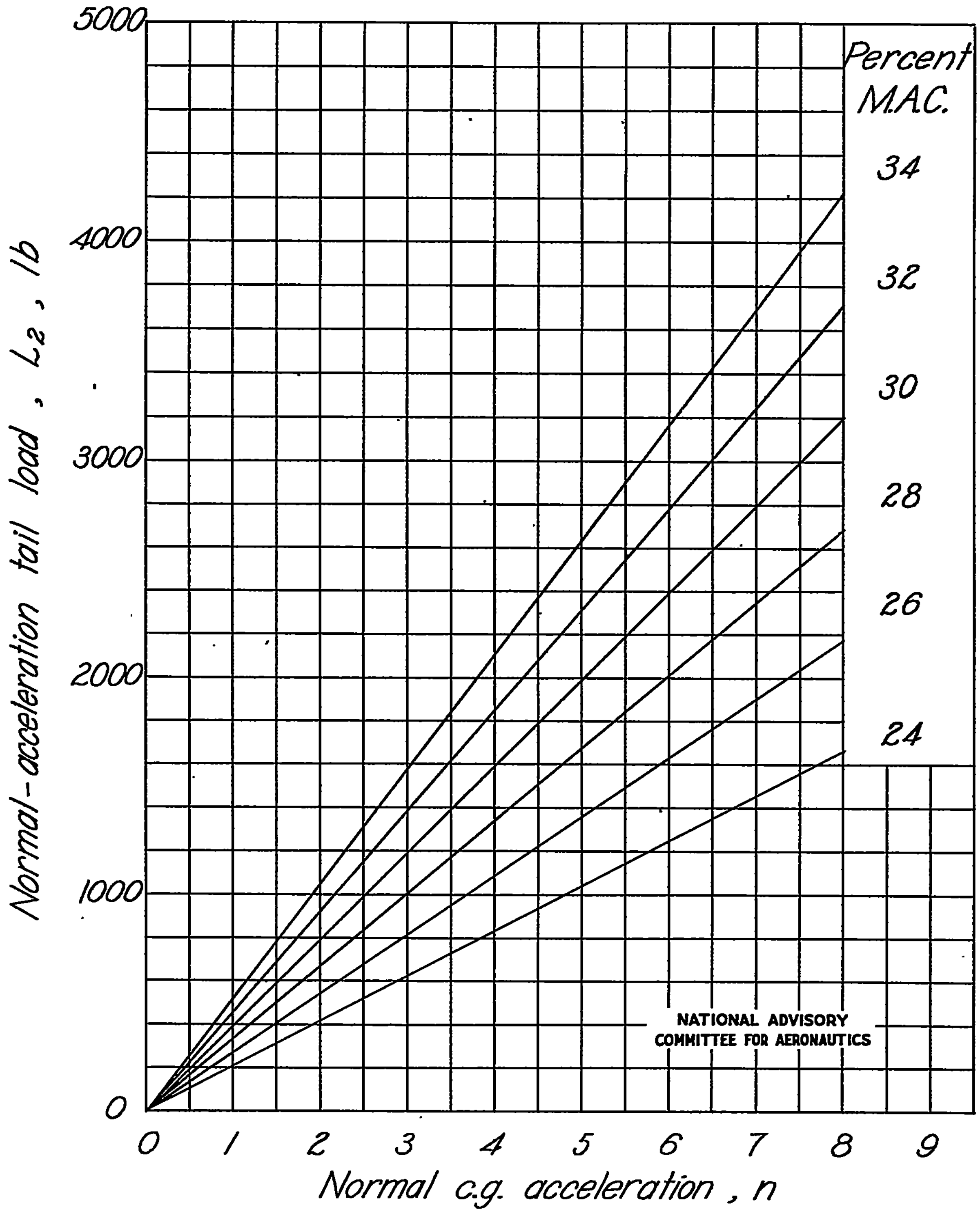

Figure 22.- Normal-acceleration tail loads for test airplane for several center-of-gravity positions.

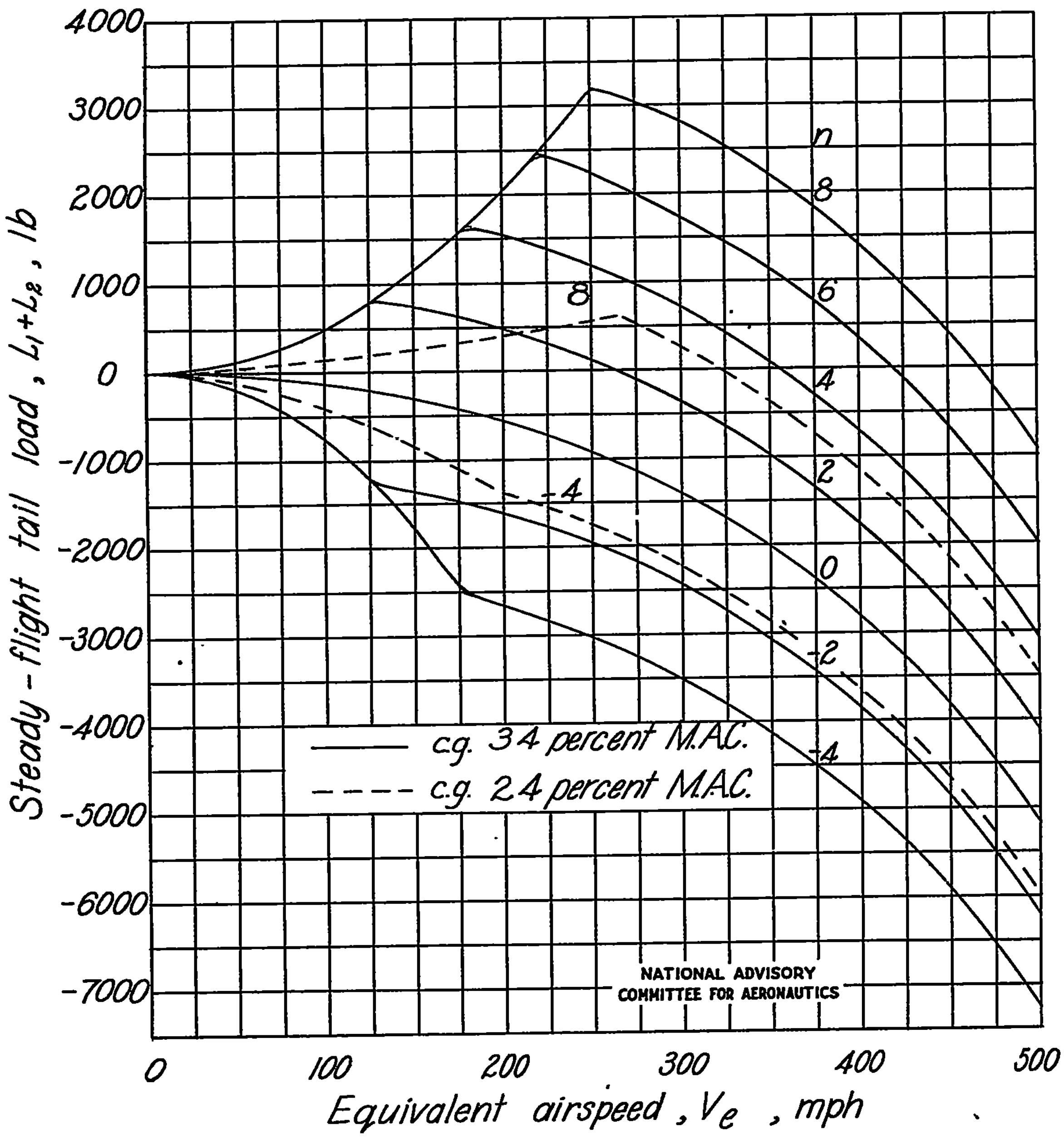

Figure 23.- Horizontal-tail loads for test airplane in steady power-off flight at sea level.

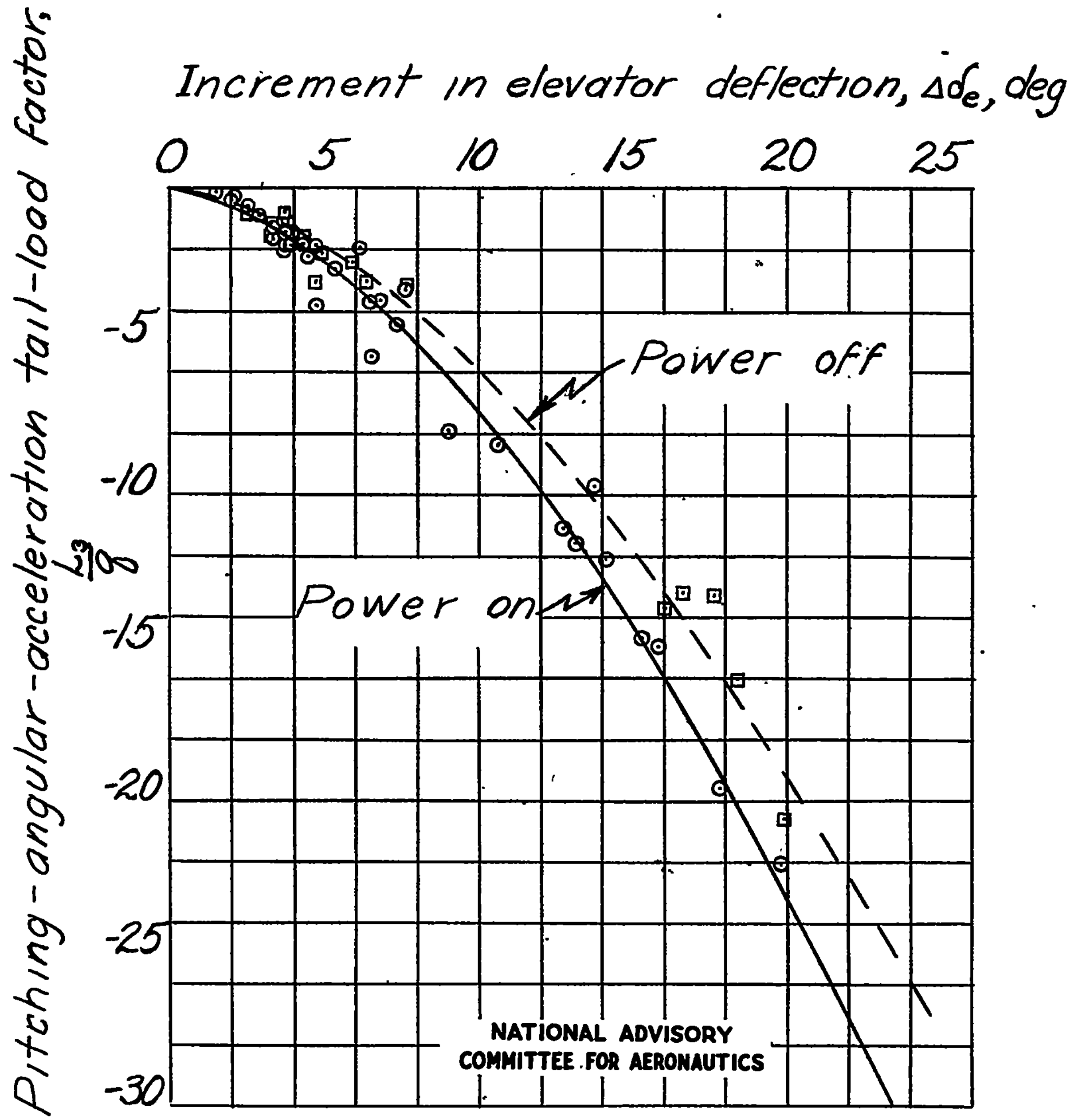

Figure 24.- Pitching-angular-acceleration tail-load-factor variation with increment in elevator deflection for all pull-ups.

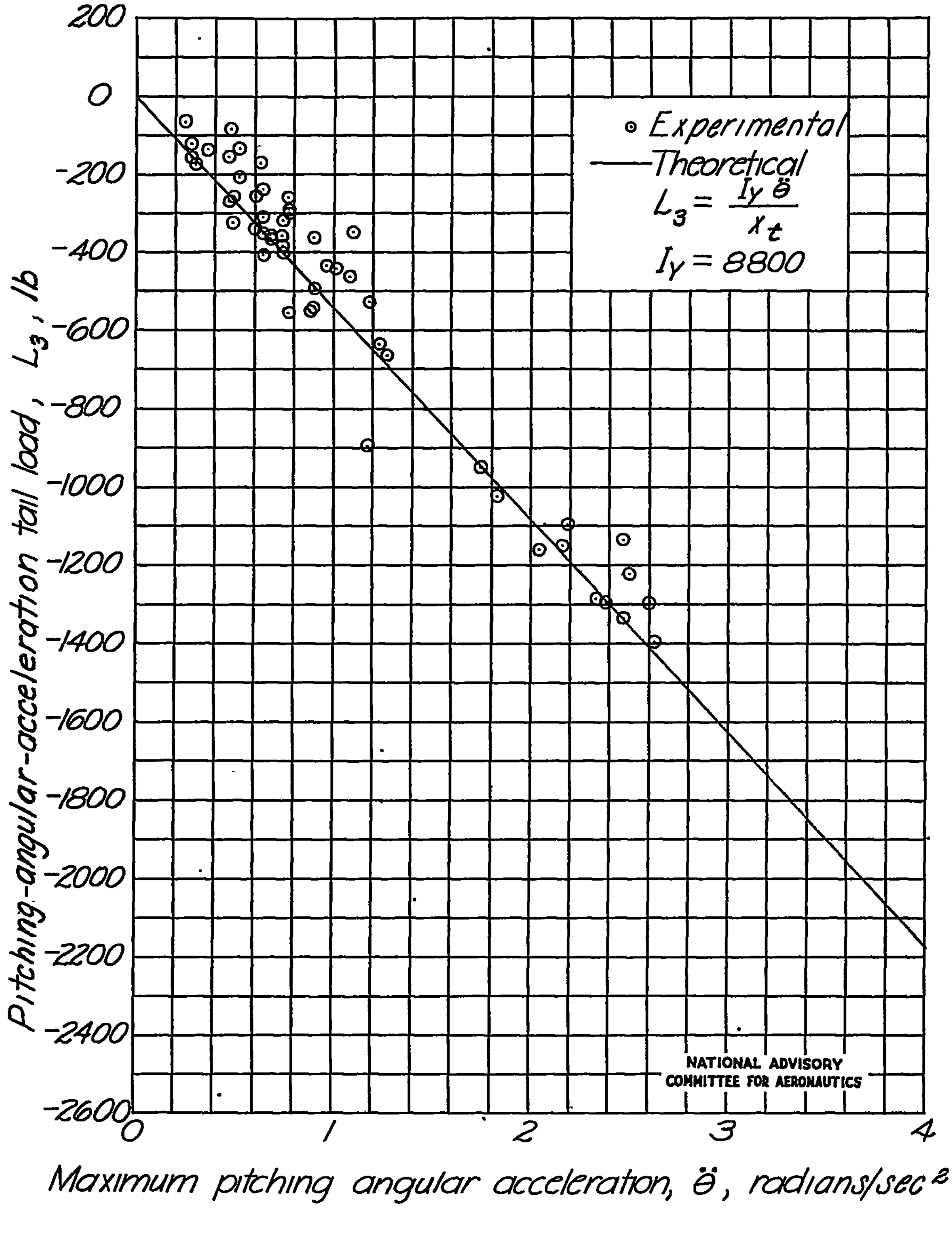

Figure 25.- Variation of pitching-angular-acceleration tail load with pitching angular acceleration for all pull-up maneuvers.

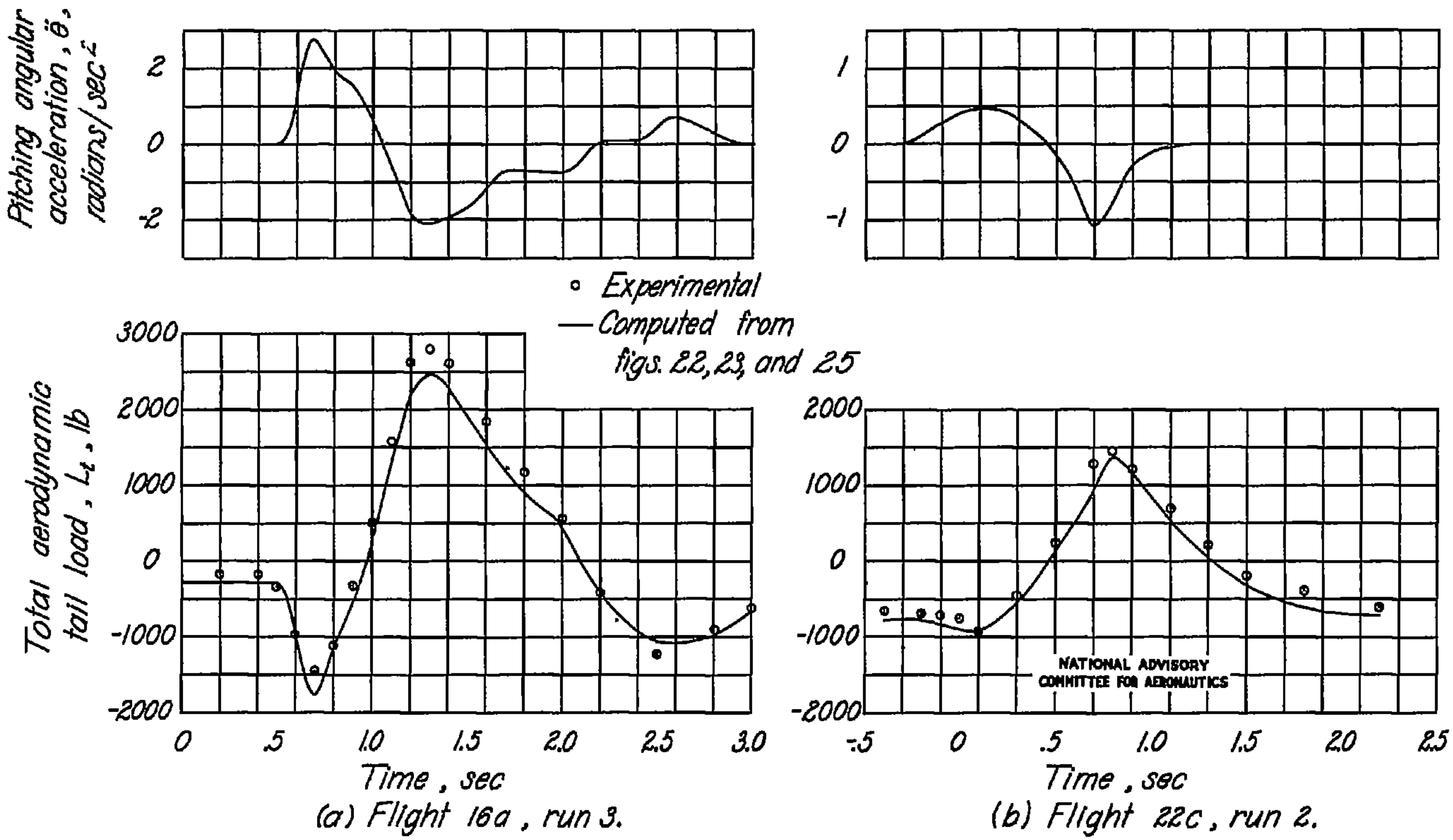

Figure 26.- Pitching-angular-acceleration time variations and a comparison of computed and measured tail loads on the test airplane.

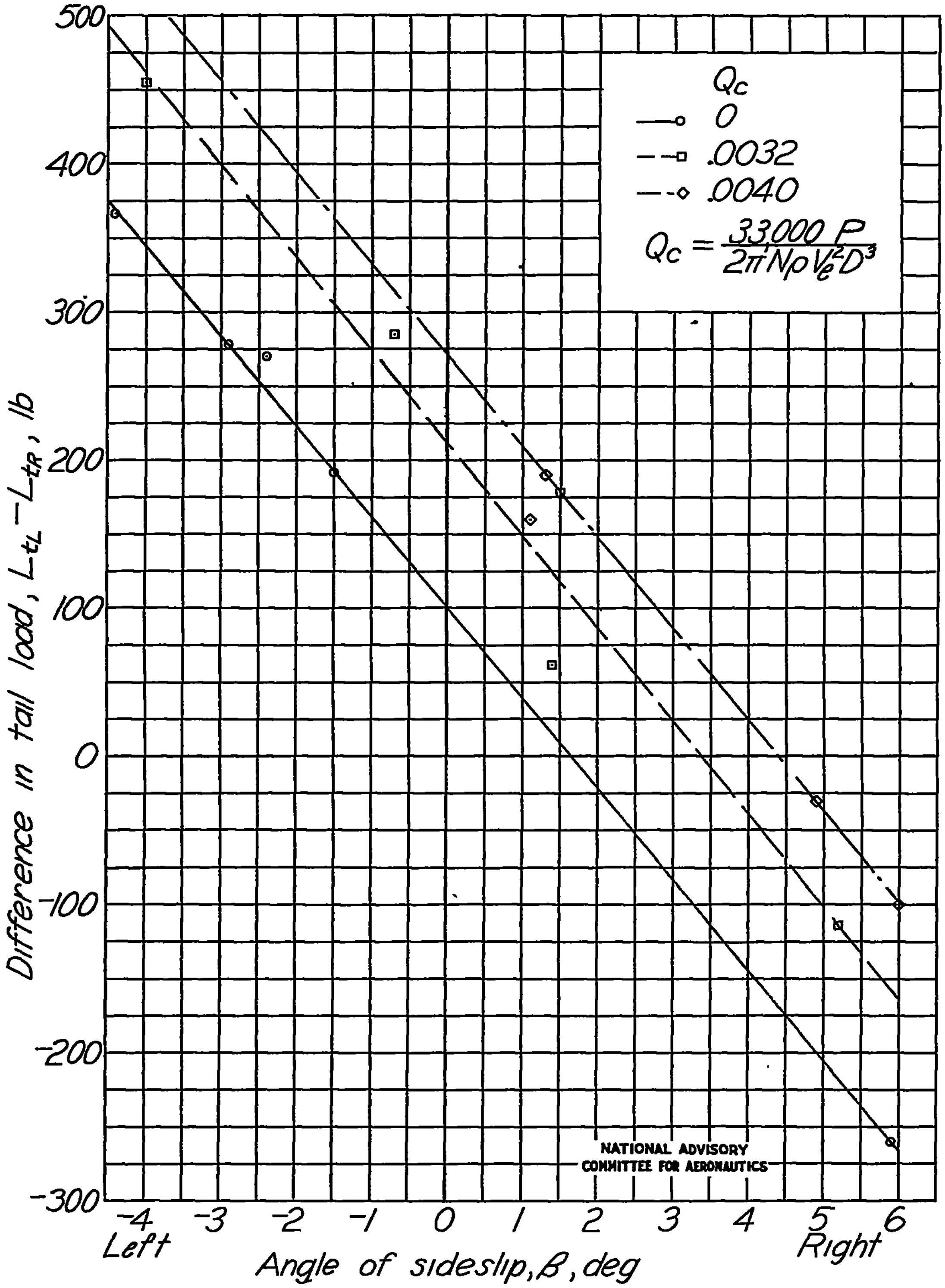

Figure 27.- Variation of load dissymmetry over horizontal tail of test airplane with sideslip and torque coefficient at approximately $0.20C_L$.

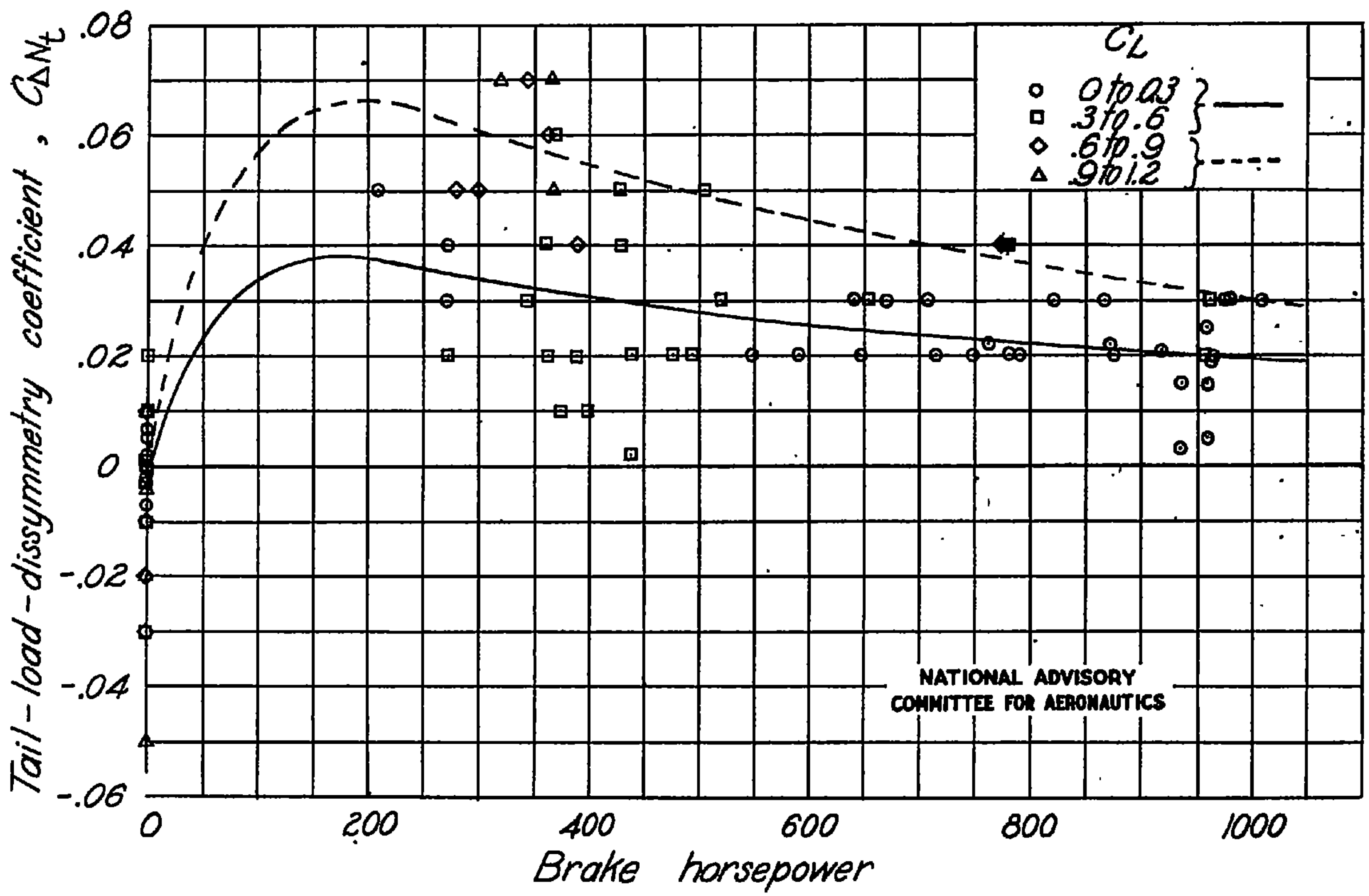

Figure 28.- Variation of tail-load-dissymmetry coefficient with engine horsepower for the test airplane.